# Highlights

**Accurate Foil Target Polarization for the Møller Polarimeter in Hall A at Jefferson Lab Utilizing World Data on Magnetization and $g'$ for pure Fe and Ni**

D. C. Jones, J. Napolitano, W. Henry, D. G. Gaskell, D. E. King, P. Souder, K. Paschke

- Research highlight 1
- Research highlight 2

# Accurate Foil Target Polarization for the Møller Polarimeter in Hall A at Jefferson Lab Utilizing World Data on Magnetization and $g'$ for pure Fe and Ni

D. C. Jones[a,*], J. Napolitano[a], W. Henry[b], D. G. Gaskell[b], D. E. King[c], P. Souder[c], K. Paschke[d]

[a] *Temple University, Philadelphia, PA, 19122*
[b] *Jefferson Lab, Newport News, VA 23606*
[c] *Syracuse University, Syracuse, NY 13244*
[d] *University of Virginia, Charlottesville, VA 22903*

**Abstract**

The Møller polarimeter in Hall A at Jefferson Lab in Newport News, VA, has provided reliable measurements of electron beam polarization for the past two decades. Past experiments have typically required polarimetry at the $\gtrsim$1% level of absolute uncertainty which the Møller polarimeter has delivered. However, the upcoming proposed experimental program including MOLLER and SoLID have stringent requirements on beam polarimetry at the level of 0.4%[1, 2], requiring a systematic rethinking of all the contributing uncertainties.

Møller polarimetry utilizes the double polarized scattering asymmetry of a polarized electron beam on a target with polarized atomic electrons. The target is a ferromagnetic material magnetized to align the spins in a given direction. In Hall A, the target is a pure iron foil aligned perpendicular to the beam and magnetized out of plane parallel or antiparallel to the beam direction. The acceptance of the detector is engineered to collect scattered electrons close to 90° in the center of mass frame where analyzing power is greatest.

One of the leading systematic errors comes from determination from calculation of the target foil polarization. This has been previously addressed in a 1997 publication "A precise target for Møller polarimetry" by deBever *et.*

*corresponding author
*Email address:* donald.jones@temple.edu (D. C. Jones)

*al* [3] at a level of precision sufficient for experiments up to this point. Several shortcomings with the previous published value require revisiting the result prior to MOLLER. This paper utilizes the existing world data to provide a best estimate for target polarization including uncertainties in magnetization, high-field and temperature dependence, and fractional contribution to magnetization from orbital effects. Uncertainties arising from imperfect target alignment and/or flatness are not addressed and remain for a future work.

*Keywords:*

---

## 1. Introduction to Møller polarimetry

As its name denotes, Møller polarimetery utilizes the analyzing power of polarized electron-electron scattering to determine the polarization of an electron beam. The polarized target is usually composed of iron or a highly ferromagnetic material. Elastically scattered events (beam electrons from atomic electrons) produce back-to-back electrons in the center of mass frame which if both detected in coincidence can be used to reduce backgrounds.

Following the analysis in [4], Møller (electron-electron) scattering at tree level in the center of mass (CM) system is given by

$$\frac{d\sigma}{d\Omega_{cm}} = \frac{\alpha^2}{s}\frac{\left(3+\cos^2\theta\right)^2}{\sin^4\theta}\Bigg[1 - P_\ell^{targ}P_\ell^{beam}A_\ell(\theta) - P_t^{targ}P_t^{beam}A_t(\theta)\cos\left(2\phi-\phi_{beam}-\phi_{targ}\right)\Bigg] \quad (1)$$

where the subscripts $T$ and $L$ refer to transverse and longitudinal polarization respectively. In the center of mass at high energy, the Mendalstam variable $s$ is equal to $(2E_{CM})^2$. The CM scattering angle is $\theta$ and the azimuthal angle of the target (beam) polarization with respect to the electron beam is $\phi_{targ(beam)}$. The analyzing powers for longitudinal and transverse polarization are given by

$$A_\ell(\theta) = \frac{(7+\cos^2\theta)\sin^2\theta}{\left(3+\cos^2\theta\right)^2} \quad \text{and} \quad A_t(\theta) = \frac{\sin^4\theta}{\left(3+\cos^2\theta\right)^2}. \quad (2)$$

$A_\ell$ is much larger than $A_t$ giving Møller polarimetery much more sensitivity to longitudinal polarization. Since $A_\ell$ is a maximum for 90 degree CM scattering

where $A_\ell = 7/9$, the optics of the Møller polarimeter in Hall A are tuned to accept events near this maximum. The Møller polarimeter in Hall A with its Fe foil polarized "out of plane" in the beam direction ($P_t^{targ} = 0$) is designed to measure the longitudinal polarization and be insensitive to the transverse polarization. Nevertheless, if the foil or magnetizing coils are not properly aligned and a transverse polarization develops, a non-negligible component of transverse asymmetry could in principle arise. In the ensuing discussion it will be assumed that the foil is properly aligned such that $P_t^{targ} = 0$ and this term will be neglected.[1]

Integrating the cross section over the acceptance of the detector gives

$$\sigma \propto 1 - P_\ell^{targ} P_\ell^{beam} A_{zz},$$

where $A_{zz} = \langle A_l(\theta) \rangle$, the acceptance-weighted analyzing power. We can now see that the left-right scattering asymmetry $A_{LR}$ is then given by

$$A_{LR} = \frac{\sigma_R - \sigma_L}{\sigma_R + \sigma_L} = P_\ell^{targ} P_\ell^{beam} A_{zz}, \tag{3}$$

where $\sigma_{L(R)}$ are the cross sections for left (right) helicity electrons.

If $A_{zz}$ and the target polarization $P_\ell^{targ}$ are known, the beam polarization can be determined from the measured scattering asymmetry.

In the approximation where the target electrons are at rest and the beam energy is large compared to the electron rest mass, $m_e$, there relationship between the lab momentum of the scattered electron, $p'$, and the center of mass scattering angle $\theta$ is given by

$$p' = \frac{p_b}{2} \left(1 + \cos\theta\right), \tag{4}$$

where $p_b$ is the electron beam momentum. Thus momentum analyzing the Møller scattered electrons also analyzes in $\theta$. Single arm Møller polarimeters leverage this characteristic to reduce potentially overwhelming Mott backgrounds. Using a narrow aperture in $\phi$ to select the scattering plane and

[1] We can approximate the relative size of this term to justify our neglect of it. Longitudinal polarization at JLab is adjusted for experiments to within 2 degrees of uncertainty, leaving a maximum $P_t^{targ}$ of 0.035. Assuming an anomalously large transverse component of the target polarization due to misalignment of 5% and a transverse analyzing power that is approximately 1/7 that of the longitudinal gives a transverse polarization contribution that is 0.025% that of the longitudinal term.

a dipole to momentum analyze the scattering events perpendicular to the scattering plane produces a characteristic Møller"stripe" downstream of the dipole. Converting to the lab scattering angle and in the absence of other focussing optics, and using the small angle approximation yield the following relationship between $\theta_{Lab}$ and momentum:

$$\theta_{Lab}^2 = 2m_e \left( \frac{p_b - p'}{p' p_b} \right). \tag{5}$$

The typical quadratic curvature of this Møller stripe is a direct result of this relationship.

### *1.1. Hall A Møller polarimeter design*

The polarimeter in Hall A is designed to take advantage of both the dipole momentum selection and the coincidence of dual arm detection to further reduce backgrounds. A simple schematic of the Hall A polarimeter is shown in Fig. 1 illustrating the key features. This polarimeter design adds to the essential elements 4 quadrupoles and an additional horizontal constraint due to the narrow apertures through the dipole. The quadrupoles are used to focus a distribution of Møller pairs roughly symmetric about the 90 degree center of mass through the dipole onto the detector. The additional focusing of the quadrupoles inverts the expected typical curvature of the Møller stripe on the detector plane as illustrated in Fig. 1.

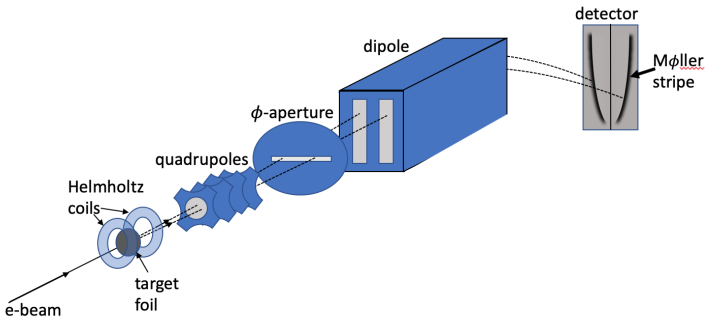


Figure 1: Simplified schematic showing the key features of the Møller polarimeter setup in Hall A. The electron beam scatters from a polarized foil target. Quadrupoles then focus the events of interest through the dipole. An aperture at the front of the dipole limits the $\phi$-acceptance defining a horizontal scattering plane. Two left-right symmetric narrow slits in the dipole momentum analyze the scattered electron pairs bending them down onto the detector plane producing characteristic Møller stripes.

## 2. Foil Target Polarization

The Møller polarimeter target consists of a set of thin foils magnetized out of plane parallel (or antiparallel) to the beam trajectory by a set of superconducting Helmholtz coils. The superconducting magnet used to polarize the target foils was built by American Magnetics Inc. The field at the center of the coils is horizontal and along the beam- line axis. The maximum field at the center is rated at 5 T at a maximum current of 93.28 A, although it is typically not run above 4 T.

The three ferromagnetic elements, Fe, Co and Ni are the obvious choices for foil targets due to their relatively high magnetization and the precision with which their magnetizations are known. The default foil of choice has thus far been pure iron since its magnetization is known with the least relative error and because it has a relatively high Curie temperature, making it less sensitive to beam heating effects.

Although the magnetization of Fe and Ni are both known to high accuracy ($\sim$ 0.2 emu/g), since the magnetization of Fe is 3 to 4 times larger, the relative error is smaller. The low Curie temperature of Ni makes it susceptible to large (percent level) corrections from target heating effects. There are fewer published measurements of high precision on Co than on the other two ferromagnetic elements.

Møller polarimetery requires finding the average target electron polariza-

| | Fe | Co | Ni |
|---|---|---|---|
| Z | 26 | 27 | 28 |
| Atomic Mass ($\mu$) | 55.845(2) | 58.933194(4) | 58.6934(4) |
| Electron Configuration | [Ar]$4s^2 3d^6$ | [Ar]$4s^2 3d^7$ | [Ar]$4s^2 3d^8$ or $4s^1 3d^9$ |
| Unpaired Electrons | 2.2 | 1.72 | 0.6 |
| Density near r.t. (g/cm$^3$) | 7.874 | 8.900 | 8.902 |
| $M_o$ at 0 K (emu/g) | 222 | 164 | 58.6 |
| $g'$ | 1.92 | 1.85 | 1.84 |
| Curie Temperature (K) | 1043 | 1400 | 631 |

Table 1: Properties of the three ferromagnetic elements.

tion; however, magnetization measures the magnetic moment of the whole atom including the orbital and spin magnetic moments. Since we only want the spin component we need to find the fraction of the magnetization that comes from spin. This is typically determined from precise measurements of the gyromagnetic ratio of an elemental sample. Thus, the final error on the target polarization will include uncertainties on both the determination of magnetization and of the spin component.

In the following sections I look at each of the three elements and determine what the total uncertainty would be if we used each of the three ferromagnetic elements as our target.

The primary issues to be dealt with are follows:

- Through the years from 1930-1980 many precise measurements have been made of the magnetization and gyromechanical properties of these elements; however, they do not necessarily agree within error. Sometimes the errors quoted are not realistic given the systematic disagreement in the data. The sources of systematic difference are often not known and yet results are averaged together and the final error quoted as the statistical variation.

- No mention is made of the nuclear contribution to the magnetic moment. The nuclear magneton is smaller than the Bohr magneton by a factor of $m_e/m_p \sim 0.05\%$. Fortunately, the main isotopes that make up iron and nickel are even-even and have spinless nuclei, but for Co the average is 4.6 nuclear magnetons making the contribution potentially above the 0.1%.

- Measurements of magnetization and gyromechanical properties are not made at the same applied field and temperature where the Møller polarimeter operates, necessitating corrections to account for these differences. The corrections must be known to sufficient accuracy and the conditions under which the measurements were taken must be known.

- Through the past century measurement of constants have become more precise and have changed. Examples of constants used in determining quoted magnetization and gyromagnetic data in the literature are the density of elements, the charge to mass ratio of the electron, and the Bohr magneton. Different groups use different values. Sometimes the values of constants used in calculations (eg. the Bohr magneton) are assumed to be known and are not given.

- Experiments measuring properties of these ferromagnetic elements used different levels of purity. It is not clear what uncertainty should be assigned to account for the effects of impurities.

- In many publications, the data are only shown as plots and the values of the measurements are not provided. The values must be subtracted with plot digitization software.

- In order to compare magnetization data taken with different sample shapes, the applied field must be converted to the internal field, $H_i$. This conversion is not always possible if the data are not given in terms of $H_i$ or the sample shape and dimensions are not provided so that this conversion can be made.

### *2.1. Determining Magnetization*

Target polarization is determined from measurements of the saturation magnetization of pure iron. Another term used in the literature is "spontaneous magnetization", which as the name implies refers to the magnetic moment of a material that spontaneously arises with no applied field. In ferromagnetic materials the magnetic moments of the electrons tend to spontaneously align in a given direction. However, due to energy considerations, domains which are small regions of aligned spin, tend to form in such a way so that the total spin averaged across many domains at the macroscopic

level is far below the saturation level and may be zero. In the presence of an applied magnetic field, the domain boundaries shift with enlarging domains with magnetic moments aligned along the direction of the field. As the applied field is increased, eventually the material will reach magnetic saturation where all the spins are aligned along the direction of the applied field. Thus, the saturation magnetization and the spontaneous magnetization are numerically equal although the spontaneous magnetization cannot be measured at room temperature due to domain formation.

Spontaneous magnetization is a function of temperature and applied field and for this reason it is often given as $M_0$, the value of saturation magnetization extrapolated to zero applied field at T = 0 K. However, experiments measure the magnetization at temperatures above 0 K with applied fields. For temperatures well below the Curie temperature and low applied fields, the magnetization has been shown to roughly follow the $T^{3/2}$ law of Bloch given as [5]

$$M_s(T) = M_0(1 - a_{3/2}T^{3/2}), \tag{6}$$

where $M_0$ is the saturation magnetization at 0 K and $a_{3/2}$ is an empirically determined constant. At higher fields and temperatures not small compared to the Curie temperature additional terms are required[6].

Pauthenet performed an extremely precise measurement of the saturation magnetization of Fe and Ni as a function of both temperature and internal field from 0 to 17 T. Pauthenet claims the absolute scale in his measurements is known only to $\pm 0.5\%$ due to uncertainty in calibration but that relative uncertainty is as the 0.01% level, making his work an authoritative reference for high field corrections. He expresses the magnetization as a function of temperature and applied field as follows:[7, 6]

$$M_s(H_i, T) = M_s(T) + A(T)H_i^{1/2} + B(T)H_i, \tag{7}$$

where $M_s$ is given by Eq 6, $H_i$ is the internal field and A(T) and B(T) are functions of temperature and can be extracted from fits to data of magnetization versus internal field at a constant temperature. Pauthenet utilizes fits to his data to give a numerical parameterization for magnetization as a function of internal magnetic field and temperature (see Eq. 9, 10 and Table 1 from [7]). Corrections for differences in temperature and internal field made will come from Eqs. 9 and 10 in [7].

It is important to note the difference between internal field and applied field. In a manner somewhat analogous to the internal electric field can-

celation inside a dielectric, the applied magnetic field is partially cancelled inside a ferromagnetic sample. This can be viewed as being caused by magnetic charges moving to the boundaries of the sample in accordance with the direction of the magnetic field. Their displacement will enhance the field outside the sample while reducing it inside. The relationship between the internal field and the applied field is given by the following equation (in the cgs system)

$$H = H_i + \frac{4\pi M}{\rho}, \tag{8}$$

where $H$ is the applied field, $H_i$ is the internal field, $M$ is the magnetization and $\rho$ is a demagnetization constant that depends on the shape of the sample. Since the internal field is thus partially cancelled by the magnetization, $4\pi M$ is sometimes referred to as the "demagnetizing field".

Well below saturation, the internal field is nearly 0 due to the demagnetizing field. In the literature, field-dependent corrections are often given as a function of internal field $H_i$ not applied field $H$. There appear to be errors in the literature that stem from incorrect exchanges of applied field and internal field. For example, Eq. 3 from deBever *et al.* incorrectly interprets Pauthenet's corrections as a function of flux density $B$ instead of internal field. As a result, they calculate a correction from an applied field of 1 T to the final value of 4 T. Their 4 T applied field translates into an internal field of $\sim$1.8 T for Fe foils, requiring a smaller correction. C. D. Graham also appears to confuse the two in Fig. 5 of [8] where he plots magnetization versus $1/H$ but combines data from multiple sources some of which are in terms of $1/H$ and others which are in terms of $1/H_i$.

Thus, the magnetization of an object at a particular temperature and applied field is not just a function of its elemental composition. Other factors that affect the magnetization are

- Shape anisotropy: the magnetization depends upon the shape of the object. Needles are very easy to magnetize along their long axis but much more difficult along a direction perpendicular to it. Each shape has a characteristic demagnetizing factor that is a function of the direction of applied field (unless symmetry dictates otherwise). Perfect spheres have a demagnetizing factor of 3. The demagnetizing factor for ellipsoids of rotation is a function of the ratio of the two axis lengths. Figure 2 shows the demagnetizing factor of ellipsoids of rotation as a function of the axis ratio where the applied magnetic field is along the

axis $R_z$. A thin foil disk such as that used in the Møller polarimeter can be taken to a flattened ellipsoid with an axis ratio of $\sim$0. In this case the demagnetizing factor approaches unity.

- Crystal anisotropy: the crystal structure of a material can create directions along which it is easier to magnetize. The direction along which magnetic saturation is reached with the smallest applied field is called the easy axis of the crystal. Monocrystalline nickel, for example, has three different magnetization axes termed the [111],[110] and [100] axes with [111] being the easy axis. Thus, if you are using monocrystalline materials, the magnitude of the external field required to reach saturation will depend upon alignment of the crystal relative to the field. For polycrystalline materials there will be no preferred direction due to crystal structure.

- Crystal structure and phase changes: some crystals have more than one possible crystal structure with different magnetizations. Their history of heating/cooling and annealing can have an effect on their magnetic properties. Cobalt, for example, goes through a phase change when heated at 690 K going from a close-packed hexagonal to a face-centered cubic crystal structure above 690 K which is unstable below that temperature. However, the exact crystal structure below 690 K (and by extension the magnetization) depends upon the grain size and the annealing process used to prepare it [9].

- Stesses and strains: stresses and strains in the material as well as porosity will affect how easily the material is magnetized. This can be seen particularly well by annealing, which often makes the material more easily magnetized[10].

Although different methods are used to measure the saturation magnetization, they broadly break down into two categories.

- Force method: a small ellipsoid sample of the element of interest is placed in a precisely determined field gradient. With a proper setup, the force on the sample by the magnetic field can be shown to be the product of the magnetization and the magnetic field gradient. Thus the magnetization is given as the force divided by the field gradient.

- Induction method: a sample is placed into a magnetic field and its presence creates a magnetic moment that is measured in pickup coils.

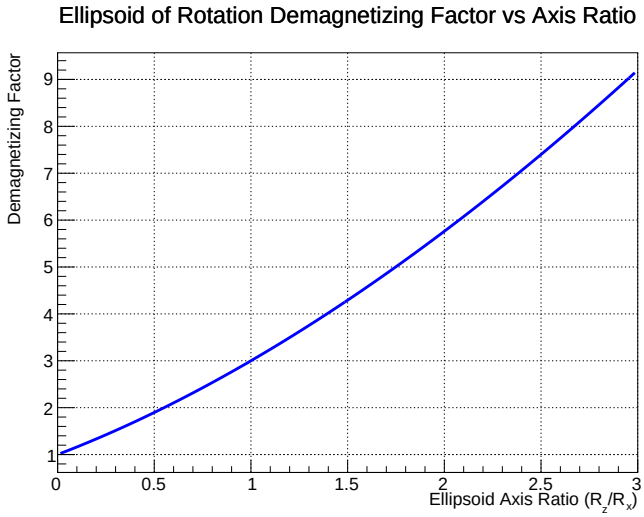


Figure 2: Demagnetizing factor for ellipoids of rotation as a function of axis ratio for external magnetic field applied along the axis of rotation $R_z$.

Although the experimental methods can be thus broadly categorized, each individual experiment takes a slightly different approach to measurement and calibration.

Measurements of magnetization are performed at a variety of applied magnetic fields and temperature and are typically expressed in terms of the saturation magnetization $M_0$ which is the extrapolation to zero applied field at 0 K[11]. A review of the literature yields many measurements of the magnetization of iron and nickel. Different approaches can be taken to obtain "consensus" values. One approach taken by H. Danan *et al.*[12] and deBever *et al.* [3] is to average the values of spontaneous magnetization $M_0(H = 0, T = 0\ K)$ and then applying a correction to obtain the magnetization at room temperature and nonzero applied fields. However, the process of extrapolation to zero field and temperature is not standardized and different methods are utilized, so it is not clear that this is a good standard for comparison. Furthermore, since we are looking for magnetization near room temperature this method introduces error extrapolating down to $M_0$ and once again correcting back up to room temperature and high fields. Since most measurements at least include data at or near room temperature and at internal fields at or close to 10000 Oe (1 T), it makes sense to utilize magnetization measurement data taken near room temperature and internal

fields of order 10 kOe. Where the available data in the literature were not available at precisely $T = 294°$K, small corrections were applied to the measurements based upon the formulation given in [7]. In each case the data of magnetization versus internal magnetic field was parameterized using Eqs. 9 and 10 from. [7]

Although the "consensus" values present here for magnetization include data from a number of measurements done over a period from 1929-2001, this is not an exhaustive data set by any means. Table 2 lists the publications used in this analysis for iron and nickel. In choosing data which data to include the following criteria were established:

- Original data was published and publication was available. Some measurements referred to in the literature are not readily available. For example much of Danan's reported measurements on Ni were never published except in his 1968 review which provides few details of the experiment. Only those data were used for which there was access to the original publication.

- Data in the publication were available near room temperature and internal field of 10 kOe. All data in this analysis were corrected to standard parameter values of $H_i = 10$ kOe and $T = 294$ K. Starting close to these values keeps the corrections small.

- Enough details were provided to obtain the internal field of the sample either because the data were given versus internal field or the demagnetizing factor could be calculated from information given.

- Sufficient information was provided about the purity of the sample used to ensure this will be a small source of error.

- Systematic errors were sufficiently small to provide useful additional information. For example, Pauthenet [7] has very precise data, but since he uses Danan's Ni data for absolute calibration, his systematic error is 0.5%. Therefore, Pauthenet's data are used for relative corrections of field and temperature, but not in the absolute measurement average. Aldred [13] also has a precise data set, but calibrates his data using the "known magnetization of nickel" which is exactly what this analysis is seeking to determine. For this reason, Aldred's data were also not utilized.

| Publication | Year | T ($^\circ K$) | Comment |
|---|---|---|---|
| Weiss and Forrer [14] | 1929 | 288 | Only Fe data used |
| R. Sanford *et al.*(NIST)[15] | 1941 | 298 | Data on Fe only |
| H. Danan [16] | 1959 | 288 | Data on Ni and Fe |
| Arajs and Dunmyre [17] | 1967 | 298 | Data on Ni and Fe |
| Crangle and Goodman [11] | 1971 | 293 | Data on Ni and Fe |
| Behrendt and Hegland (NASA)[18] | 1972 | 298.9 | Data on Fe only |
| R. Shull *et al.*(NIST) | 2000 | 298 | Data on Ni only |

Table 2: Publications used in obtaining consensus value for magnetization near room temperature at high fields.

Fig.3 shows the data for the magnetization of Fe from the published sources before and after correction to T=294°K. Where data were not given in terms of internal field $H_int$, they were converted to $H_int$ using Eq. 8 using information given in the publications to determine the demagnetizing field $4\pi M/\rho$. The data are approximately linear as expected in the high-field region above 3 kOe. The lower panel of Fig. 3 shows the data after correction to the standard temperature 294 K, which makes the spread wider. The temperature correction is taken from Pauthenet's parameterization given in Eq 9 in [7]:

$$M(T,H_i) = M_0 + aT^{3/2}F(3/2, bH_i/T) + cT^{5/2}F(5/2, bH_i/T) + \chi(T)H_i, \text{ emu/g} \quad (9)$$

where a, b and c are constants found empirically to be $a = 307 \times 10^{-6}$, $b = 1.378 \times 10^{-4}$and $c = -22.8 \times 10^{-8}$.[2] F is given by $F(s, H/T) = \sum_{p=1}^{\infty} p^{-s} e^{-pg\mu_B H/k_B T}$ with $g$ the Lande g-factor, $\mu_B$ the Bohr magneton and $k_B$ the Boltzmann constant. $\chi(T)$ is the susceptibility as a function of temperature and its evaluation is given in Table 1 of [7] for discrete values. A linear approximation $\chi(T) \approx 3.644 \times 10^{-6} + 5.0434 \times 10^{-10} T$ was obtained from a fit to the data in order to be able to evaluate $\chi(T)$ for any temperature. Pauthenet's calculated curves for various temperatures do not precisely agree with his data; however, the difference between his calculated temperature corrections and those seen empirically in his data are negligibly small

[2]Note that Pauthenet uses $b = 1.378$ for Fe in Eq. 9 of [7] and $b = 1.478$ for Ni in Eq. 10 of [7], but the only way I could replicate his plots in Figure 1 of [7] and [6] was to use $b = 1.378 \times 10^{-4}$ for Fe and $b = 1.478 \times 10^{-4}$ for Ni.

over the ±6°C correction required in this analysis.

To get an average parameterization versus internal field, each of the six temperature-corrected data sets were fit individually using Pauthenet's parameterization in Eq. 9 with $T = 294\ K$ as can be seen in Fig. 4. Pauthenet's work was chosen as the high-field reference since he quotes the relative uncertainty of the data used in his fit to be at the 0.01% level. Although his temperature parameterization appears to miss slightly, the overall shape of his curves versus internal field appear to represent the data to high precision. In particular, the slopes of the high-field quasi-linear region appear to agree well between data and the parameterized fits. An additional term of $a/H_{int}^2$ was added to Pauthenet's parameterization to provide a better fit in the roll-off region at low field. Pauthenet's data did not roll off as quickly as the data used here (see Fig. 1 of [7]). He explains the curvature at low field in his data to be consistent with the effect of the field on spin-waves. However, the exact curvature in this region is expected to depend on the composition, purity in addition to stresses and imperfections in the sample used. Pauthenet used a high purity monocrystalline sample, whereas many of the datasets included here used polycrystalline samples, so perhaps it is not surprising to see a discrepancy in this region. Stoner discusses the interpretation of terms proportional to $1/H_{int}$ as arising from inclusions (impurities or cavities) in the sample and $1/H_{int}^2$ as arising from stresses and imperfections (see discussion around Eqs. 4.18-4.22 in [19] and around Eq. 7 of [20]). For the Fe datasets included here, the term proportional to $1/H_{int}$ was not needed, so only a term of the form $a/H_{int}^2$ was retained. The coefficient $a$ was constrained to values 0 or below in the fit to maintain consistency with the physics model. Note that the data for Weiss and Forrer and for Sanford (NASA) *et al.* are condensed in the literature to a single value of $H_{int}$ even though they are composed of multiple values across a range of applied fields not included in the publication. Since it does not make sense to fit these to the full parameterization, only $M_0$ was allowed to float in the fit such that the curve went through the single point and the parameter $a$ was assigned the average value of the other four data sets where it was used as a fit parameter. The average value of $M_0$ and $a$ from the fits were used to produce the "Average" parameterization curve. To within 0.01 emu/g over the range of $H_{int}$ from 8 to 28 kOe (about 3 to 5T applied field for a thin Fe foil magnetized out of plane normal to the surface) the following polynomial parametrization is

valid:

$$M(H_{int}, 294\ K) = 217.606 + 2.7836 \times 10^{-5} H_{int} - 2.6223 \times 10^{-10} H_{int}. \quad (10)$$

This parameterization is shown in Fig.5. A systematic error band of ±0.20% is assigned to account for the spread of the data. The source of this systematic spread across the datasets is not clear.

Since the saturation magnetization of iron is approximately 2.2 T and the demagnetization factor is unity for a thin foil magnetized out of plane, the internal field is approximately 2.2 T less than the applied field near saturation. Thus a uniform external 4 T magnetic field corresponds to an internal field of approximately 1.8 T. Converting Eq. 10 to applied field $H$ in Tesla for the specific case of a thin foil magnetized out of plane gives a second order parameterization that is within ±0.01 emu/g of the fit curve over the region 3-5 T applied field:

$$M(emu/g) = 216.867 + 0.393741 H^2 + 0.026223 H^2. \quad (11)$$

This gives the magnetization per gram for iron at 294°K with an applied field of 4 T as $\sigma_{Fe} = 218.02 \pm 0.39$ emu/g. This translates into $2.1800 \pm 0.0039\ \mu_B$/atom which differs by 0.14% from the value of $2.183 \pm 0.002\ \mu_B$/atom determined by deBever *et al.*[3] partially due to their over-correction for the magnetic field dependence.

A similar analysis of the literature for nickel is shown in Figs. 3 to 5. Like for Fe, the Ni data was fit to the Pauthenet parameterization with an additional term of $a/H_{int}$. Each of the four data sets were fit independently in $M_0$ and $a$ with $a$ being constrained to be 0 or less as before. The only exception to this parameterization was the Crangle data set where $a$ was fixed at 0 since there were no low field data to guide the fit. The fits are shown in Fig. **??**. The "Average" parameterization curve was formed using the average $M_0$ and $a$ from the fits. This average parameterization along with a proposed systematic error band of ±0.2% or 0.11 emu/g is shown in Fig 8. Since the saturation magnetization of nickel is approximately 0.6 T and the demagnetization factor is unity for a thin foil magnetized out of plane, the internal field is approximately 0.6 T less than the applied field near saturation. Thus a uniform external 2 T magnetic field corresponds to an internal field of approximately 1.4 T. Reading from Fig. 5 gives the magnetization per gram for nickel at 294°K with an applied field of 2 T as $\sigma_{Ni} = 55.24 \pm 0.11$ emu/g, which translates into $0.5806 \pm 0.0012\ \mu_B$/atom.

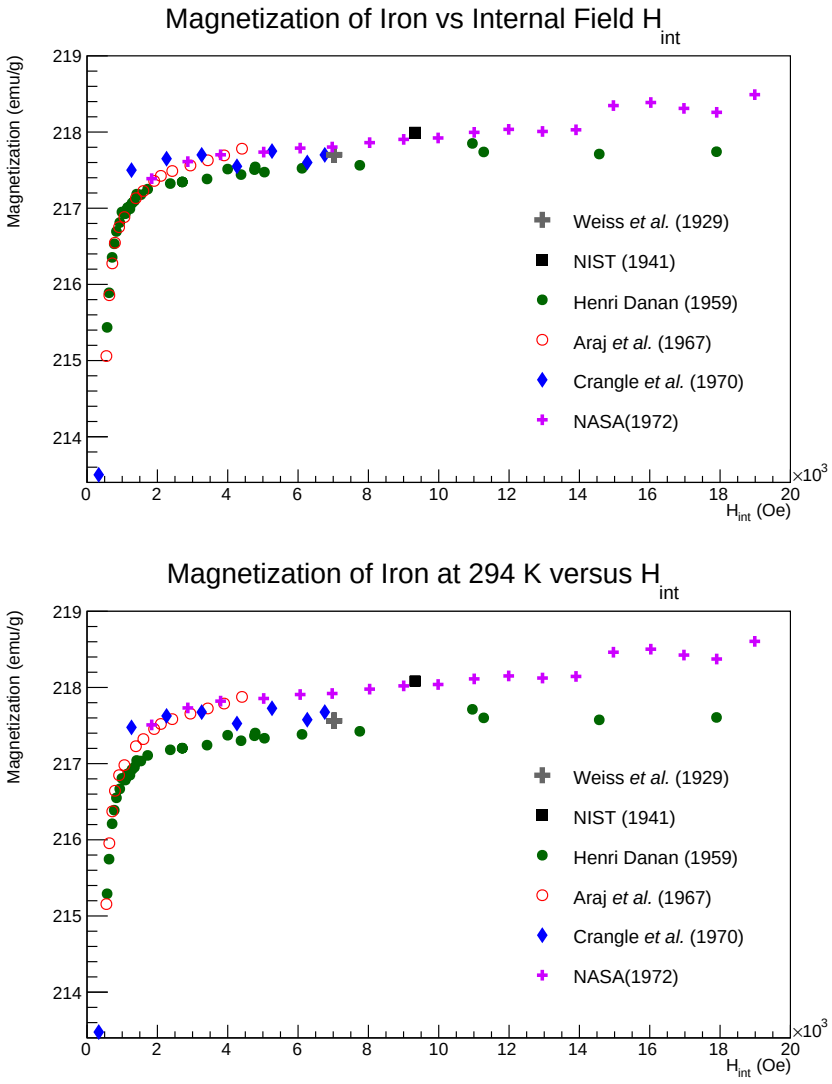


Figure 3: Published magnetization data from various sources for Fe shown versus internal field. The top plot shows data for temperature at which it was taken and the the bottom plot shows the same data corrected to 294°K.

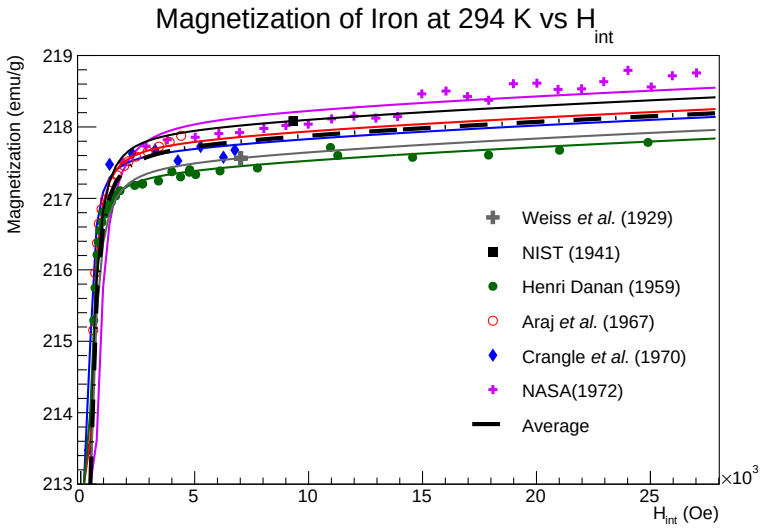


Figure 4: Fits to magnetization data using a modified form of Eq. 9 from [7] (see text). Each of the six datasets are fit individually and the resulting averaged as detailed in the text.

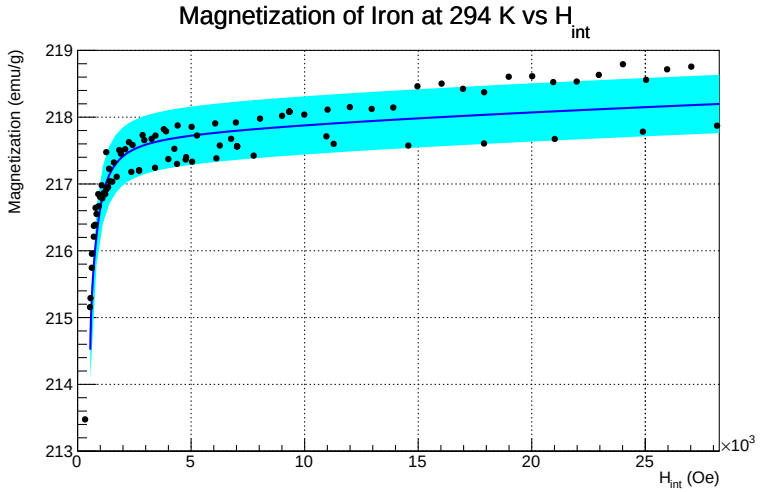


Figure 5: Published magnetization data from various sources for Fe plotted versus internal field corrected to 294°K and shown with proposed parametrization curve for internal fields up to 29 kOe (2.9 T). The error band corresponds to 0.20% or ∼0.44 emu/g

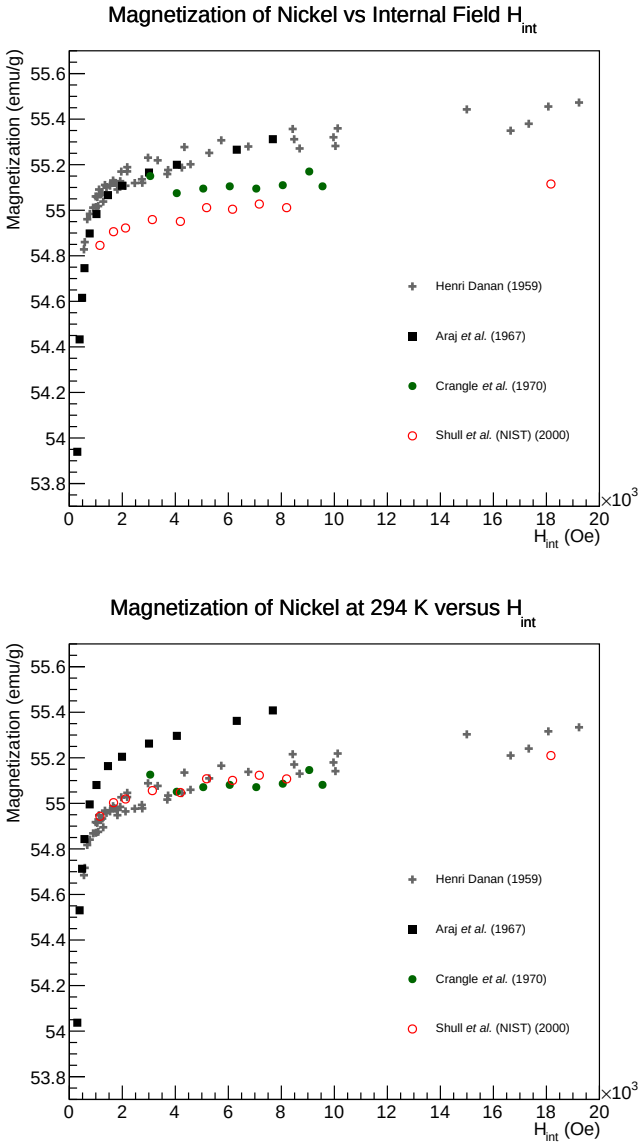


Figure 6: Published magnetization data from various source for Ni shown versus internal field. The top plot shows data for temperature at which it was taken and the the bottom plot shows the same data corrected to 294°K. There is good agreement in the data with the clear exception of that from Arajs *et al.* which are systematically higher by $\sim 0.5\%$. The reason for this discrepancy is not clear, although their publication only claims 0.2% accuracy for saturation magnetization which could partially explain the difference.

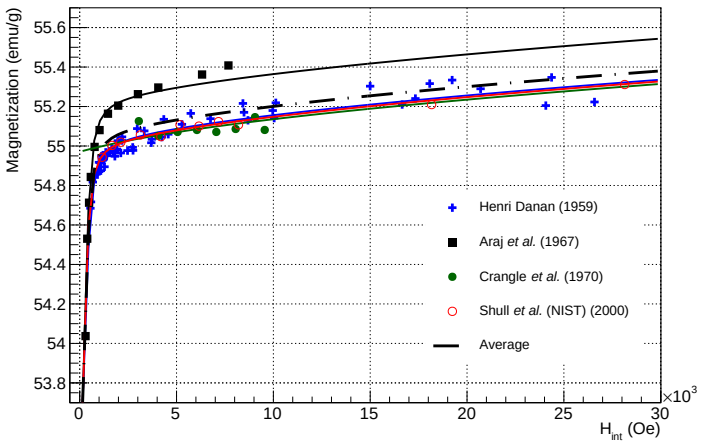


Figure 7: Fits to Ni magnetization datasets using a modified form of Eq. 10 from (see text).[7]. The "Average" curve is formed from the average fit parameters.

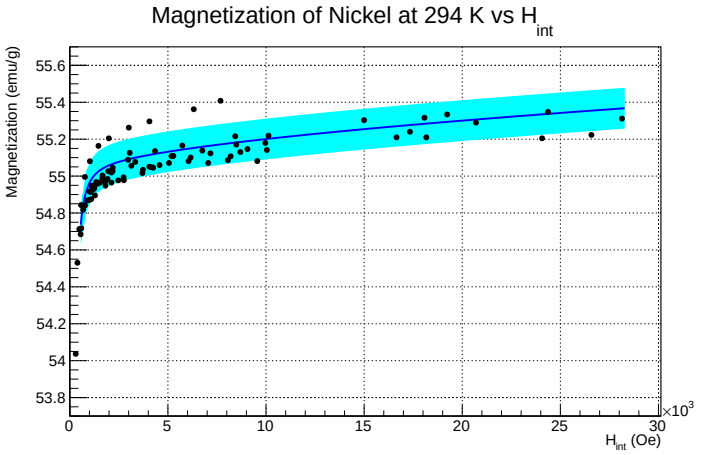


Figure 8: Published magnetization data from various sources for Ni plotted versus internal field corrected to 294°K and shown with proposed parametrization curve for internal fields up to 20 kOe (2 T). The curve is the "Average" curve from Fig. 7 which is simply the parametrization with the average fit parameter values. For a thin nickel foil magnetized out of plane (normal to the surface) close to saturation, the difference between the internal and applied field is about 0.6 T so 2 T external field corresponds to 1.4 T internal field. The error band corresponds to 0.20% or ∼0.11 emu/g.

*2.1.1. Magnetocrystalline anisotropy and Co*

As previously mentioned, the crystal structure of ferromagnetic elements creates axes along which it is easier or harder to magnetize the material. The origin of this anisoptropy is nicely explained by a quote from *An Introduction to Magnetic Materials* by Cullity and Graham [21]:

> Crystal anisotropy is due mainly to spin-orbit coupling. By coupling is meant a kind of interaction. Thus we can speak of the exchange interaction between two neighboring spins as a spin-spin coupling. This coupling can be very strong, and acts to keep neighboring spins parallel or antiparallel to one another. But the associated exchange energy is isotropic; it depends only on the angle between adjacent spins, as stated by Equation 4.29, and not at all on the direction of the spin axis relative to the crystal lattice. The spin-spin coupling therefore cannot contribute to the crystal anisotropy.
>
> The orbit-lattice coupling is also strong. This follows from the fact that orbital magnetic moments are almost entirely quenched, as discussed in Section 3.7. This means, in effect, that the orientations of the orbits are fixed very strongly to the lattice, because even large fields cannot change them.
>
> There is also a coupling between the spin and the orbital motion of each electron. When an external field tries to reorient the spin of an electron, the orbit of that electron also tends to be reoriented. But the orbit is strongly coupled to the lattice and therefore resists the attempt to rotate the spin axis. The energy required to rotate the spin system of a domain away from the easy direction, which we call the anisotropy energy, is just the energy required to overcome the spin-orbit coupling. This coupling is relatively weak, because fields of a few hundred oersteds or a few tens of kilamps per meter are usually strong enough to rotate the spins. Inasmuch as the lattice consists of a number of atomic nuclei arranged in space, each with its surrounding cloud of orbital electrons, we can also speak of a spin-lattice coupling and conclude that it too is weak.

Iron and nickel (iron is body-centered cubic and nickel is face-centered cubic) have hard, medium and easy magnetization axes due to their crys-

tal lattice structure. Magnetization along any axis other than the easy axis requires a larger applied magnetic field due to the anisotropy energy. The plots in Fig. 9 show the magnetization curves for iron and nickel along each of their magnetocrystalline axes. It is interesting that each of the magnetization curves in Fig 9 appears to approach the same saturation magnetization. Pauthenet measures the saturation magnetization with precision along the different crystallographic axes for Ni and Fe and concludes that the saturation magnetization is the same [6].

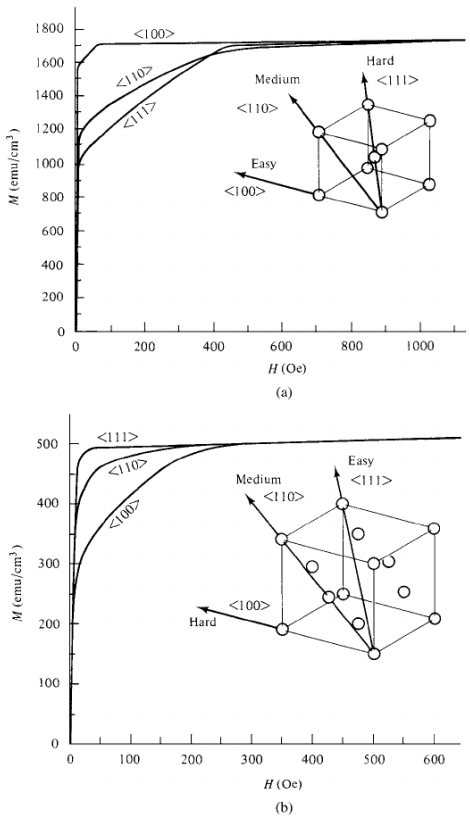


Figure 9: Magnetization curves for single crystals of Fe (a) and Ni (b) demonstrating the relative difficulty of magnetizing the crystals along different directions. (Figure taken from [21].)

The crystal structure of cobalt (close-packed hexagonal at room temperature) creates a greater magnetocrystalline anisotropy than it does for the other two ferromagnetic elements. Cobalt has an easy axis of magnetization

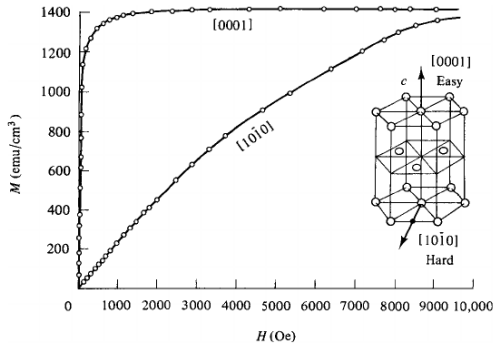


Figure 10: Magnetization curves Co demonstrating the relative difficulty of magnetizing the crystal along different directions. (Figure taken from [21].)

and a hard axis perpendicular to the easy axis as can be seen in Fig. 10 taken from [21]. What is striking about these magnetization curves is how difficult it is to magnetize cobalt along its hard axes. A feature not apparent from the $\sim$1 T applied field in Fig. 10 is that the saturation magnetization is different along the easy and hard axes. Pauthenet measured this difference to be at the 0.5% level in his careful study of magnetization versus field[6]. In a polycrystalline sample such as a foil that might be utilized in the Møller polarimeter, it is not apparent how to determine the saturation magnetization. Perhaps it is close enough to average the magnetization curves with twice the weighting on the hard axis value to account for the two orthogonal axes perpendicular to the single easy axis. It is also not apparent how high a field would be required to saturate a cobalt foil normal to its surface.

At temperatures above 690°K the crystal structure of Co becomes face-centered cubic, whereas below that it transitions to close-packed hexagonal. According to Owen *et. al*, the crystal structure of polycrystalline cobalt will typically be a mixture of face-centered and close-packed hexagonal crystals[9]. In any case, given the uncertainties for determining the magnetization for cobalt, its value as a target foil is greatly diminished below the 1% level. Quoting from Myers and Sucksmith [22]

> On account of the large magnetic anisotropy of hexagonal cobalt and the random orientation of the crystal grains, no reliable values of saturation magnetization can be obtained from the measurements on polycrystalline cobalt at and below room temperature, the magnetic anisotropy becoming more pronounced at

> lower temperatures. Furthermore, it has been shown be many workers, in particular, Edwards & Lipson (1943) and Toiano & Tokich (1948), that polycrystalline cobalt at room temperature is often of mixed-phase content possessing close-packed hexagonal and face-centered cubic structures both being present. Hence apart from the difficulty of magnetization of cobalt, the fact that the two phases of cobalt may co-exist make the significance of some of the results obtained by Wiess & Forrer (1929) and by Allen & Constant (1933) very uncertain.

The reasons for not using cobalt target foils are summarized below.

- Large systematic error on magnetization. The best data the authors found for the magnetization of cobalt was taken by Pauthenet (see Fig. 3 in [7]), for which he quotes a systematic error of 0.5%.
- Magnetic anisotropy. The magnetic anisotropy of cobalt creates a magnetization that is axis dependent with magnetization values along the hard and easy axes that are different at the 0.5% level. It is not clear how to choose the value for polycrystalline cobalt.
- Crystal structure uncertainty. The crystal structure of cobalt may vary from sample to sample and may depend on the annealing process or history of heating/cooling. This will create differences in saturation magnetization from sample to sample.
- Source of anisotropy. It is not known if the anisotropy in saturation magnetization is caused primarily by the orbital or spin which adds an additional uncertainty in determining the fraction of magnetization from the spin.

*2.1.2. Target heating and temperature corrections*

When the electron beam is on target during a Møller polarimetry measurement, the foil heats up a few tens of degrees. Since there is a slight temperature dependence to the magnetization a correction will have to be applied. The further from the Curie temperature of the material, the smaller the correction will be. Therefore, we can expect the beam heating correction for Ni to be higher than that of Fe. In the absence of a direct way of determining the temperature of the foil at the beam spot during operation or of monitoring the relative magnetization *in situ*, an estimate of the temperature increase must be made. This section provides a calculation of the foil heating from the electron beam under a set of assumptions.

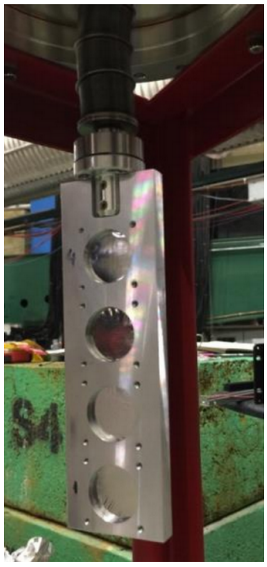

Figure 11: Target ladder with four thin iron foil disks. The support structure is aluminum.

The thin foil disks used in the Møller polarimeter are a few microns thick and circular(see Fig. 11). The electron beam is approximately centered on the target disk during operation to avoid scattering off the aluminum ladder. The electron beam is approximately Gaussian with a 1 $\sigma$ diameter of 90 $\mu$m give or take a few tens of microns. The beam is not typically rastered on the Møller target but has a natural helicity-correlated jitter of a few tens of microns.

- The beam introduces a heat load that is approximately a circular Gaussian distribution centered on the foil disk.
- Radiative black-body cooling is negligible.
- The aluminum frame constitutes an approximately infinite heat sink i.e. the temperature of the aluminum frame remains at or near room temperature.
- The foils are 0.5 inch in diameter and in perfect thermal contact with the aluminum frame.

The heat equation for this situation with only radial dependence and in the

steady state is given as

$$\kappa \nabla^2 T = -\rho \alpha B_{flux} \tag{12}$$

$$\frac{\kappa}{r}\frac{\partial}{\partial r}\left(r\frac{\partial T}{\partial r}\right) = -\rho \alpha B_{flux} \tag{13}$$

$$\frac{\partial}{\partial r}\left(r\frac{\partial T}{\partial r}\right) = -\frac{\rho \alpha}{\kappa} r B_{flux}, \tag{14}$$

where $\kappa$ is the temperature dependent thermal conductivity of Fe which is approximately 0.8 W/(K cm) at room temperature, $\rho = 7.87$ g/cm$^3$ is the density of Fe, and $\alpha$ is the collision stopping power for electrons in Fe, which is a function of electron energy. $B_{flux} = \frac{d^3 N_e}{dsdt}$ is the flux density of the beam in $e^-$/(cm$^2$ s). This equation can be easily solved numerically with a Gaussian beam profile $B_{flux} = \frac{I}{1.6\times10^{-19}\left(2\pi r_b^2\right)} e^{-r^2/2r_b^2}$, where $r_{beam}^2 = \sigma_x^2 + \sigma_y^2$ is the 1 $\sigma$ radius of the beam. The solution is shown in Fig. 12 with a 1 $\mu A$ beam heat load with $r_{beam} = 150$ $\mu$m. Using these data we get 11 °C/$\mu$A. A similar temperature rise is found for Ni foil. The temperature dependence of magnetization for iron and nickel from [7, 6] yields the sensitivity shown in Fig. 13. The model was evaluated for applied fields of 2 T for nickel and 4 T for iron. A linear fit to the region of interest for heating from an electron beam between 0.5 and 1.5 $\mu$A yields slopes of -0.025 (emu/g/°C) for Ni and -0.024 (emu/g/°C) for Fe. A conservative uncertainty of 30% gives an uncertainty in the magnetization of $\pm$0.08 (emu/g/$\mu$A) for both Ni and Fe.

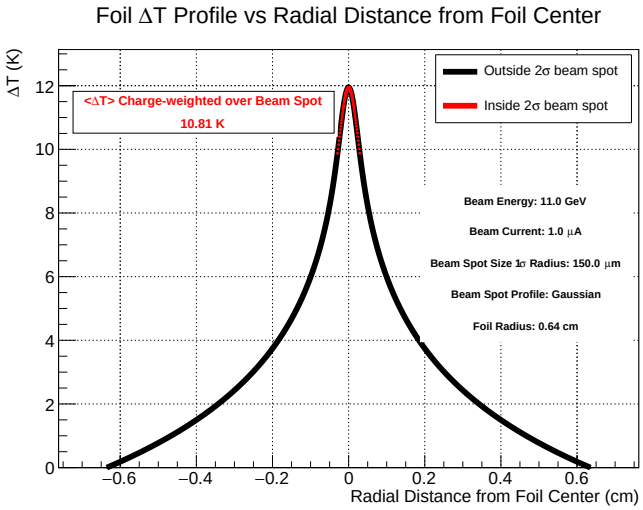


Figure 12: Foil temperature distribution in a 0.5 inch diameter foil under a 1 $\mu$A beam load. The electron beam is assumed to have a Gaussian distribution with a $1\sigma$ radius $r_{beam} = 150$ $\mu$m. The red tip of the distribution is the part of the foil inside the $2\sigma$ beam spot. The maximum temperature rise is 12 K above the temperature of the aluminum frame and the average temperature rise weighted by the beam distribution over the beam spot is 10.8 K. The ROOT macro for making this plot is called "FeFoilHeating.C" and is available at the following Git repository: https://github.com/jonesdc76/MollerPolarimetry/blob/master/TargetPolarization/

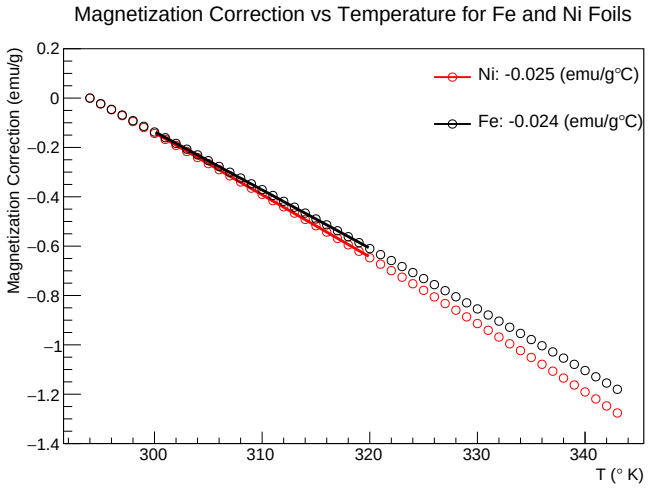


Figure 13: Temperature correction as a function of temperature above room temperature (assumed to be 294 K) for nickel and iron using the model in [7, 6]. The model was evaluated for applied fields of 2 T for nickel and 4 T for iron. The fits are over the temperature range 300 to 320 °K.

*2.1.3. Effect of impurities*

This section looks at the effect of impurities on the measured magnetization. The experiments whose data are used in this analysis (with the possible exception of the measurement at NASA by Behrendt *et al.*) utilized highly pure Fe and Ni samples. Table 3 lists the level of impurities in the samples used in the various experiments whose data are used in this analysis. Although Weiss and Forrer [14] do not give a numerical value for the level of impurities they assure us that there were no impurities at a measurable level. They used this highly pure sample for the most precise results and many samples of less pure iron for less accurate studies. The less pure sample had a total of 0.22% impurities with 0.09% of that being carbon. Since hundreds of ppm were easily measured we can be assured that the pure sample was much better than this. Although the NASA measurement by Behrendt *et al.* does not list a purity level for the sample, given the reputation and quality of science from this institution combined with the fact that they were verifying past measurements for pure iron, it is difficult to believe they would utilize a sample with >0.1% impurities. Generally speaking, addition of non-ferromagnetic impurities decreases the magnetization (see for example [26, 27, 15]). Sanford *et al.* corrected for the effect of $\sim 0.01\%$ impurities which yielded a correction at the $\sim 0.02\%$ level[15]. Ahern *et al.* also found that adding copper to nickel reduced the magnetization by about

Table 3: Level of impurities from the various measurements used in this analysis.

| Experiment | Element | Impurity Fraction |
|---|---|---|
| Weiss and Forrer [14] | Fe | "No detectable impurities" |
| R. Sanford *et al.*(NIST)[15] | Fe | <0.01% |
| H. Danan [16, 12] | Fe | Same as Weiss and Forrer |
| Arajs and Dunmyre [23][17] | Fe | ∼600 ppm |
| Crangle and Goodman [11] | Fe | 0.06% and 0.006% |
| Behrendt and Hegland (NASA)[18] | Fe | Not given |
| H. Danan [16, 12] | Ni | 0.01% |
| Arajs and Dunmyre [24, 25, 17] | Ni | ∼30 ppm |
| Crangle and Goodman [11] | Ni | 0.05% and 0.005% |
| R. Shull *et al.*(NIST) | Ni | 10 ppm |

2% for every 1% of the nickel replaced by copper. Using the assumption of magnetization being reduced by about 2% for every 1% of impurities to set the scale for our uncertainty, we see that the largest error (0.12%) would be in the Arajs and Dunmyre data on iron. Given the purity of the data samples and the systematic error already assigned from the spread in the data, it seems safe to assume that the error from impurities in the determination of magnetization for Fe and Ni is negligible. We will revisit impurities once again in the determination of the spin component of the magnetization.

Another source of impurities generally not accounted for in assays is the surface oxidation. Iron oxides such as $Fe_3O_4$, have a much smaller magnetization than pure Fe. Alex Gray, a physics professor at Temple University agreed to take XMCD measurements of one of our pure Fe foils at the Advanced Light Source. This measurement only probed the first few nanometers of the foil, but there was evidence of oxides on the surface although it looked shiny and clean. In private communication, Alex confirmed that it is usual to have a couple of nanometers of oxidation on the surface of Fe samples that were not properly cleaned. This suggests that foils nearing micron level thickness will have surface contamination from oxides at the 0.1% level. To make this uncertainty negligible it is recommended to utlize foils 10 $\mu$m or thicker. This, of course, does not include a more difficult to quantify level of oxidation inside the foil resulting from the method in which it is manufactured (eg. rolled or pressed).

*2.1.4. Nuclear contribution to the magnetic moment*

Discussion of the nuclear contribution to the magnetic moment appears to be absent from the literature on magnetization measurements. This is most likely due to the suppression of the nuclear magneton relative to the Bohr magneton by the electron to proton mass ratio ($\mu_B/\mu_N = m_e/m_p$), a factor of about 1/2000. However, in the determination of target polarization for the Møller polarimeter, effects at the 0.1% level require consideration. In the nucleus spins are paired in such a way that all even-even nuclei have zero spin. Fortunately for us, the isotopic distribution of iron (26 protons) is such that 97.9% of natural iron is from even-even isotopes. The single even-odd naturally occuring isotope $^{57}$Fe has a negligible nuclear spin of $0.09\mu_N$[28]. For nickel (28 protons) the situation is also favorable with natural nickel being composed of 98.9% even-even isotopes. This gives us another two orders of magnitude suppression and renders the nuclear spin contribution completely negligible. However, for cobalt (27 protons), the only stable isotope has a

nuclear spin of 4.63 $\mu_N$, potentially creating errors at the 0.2% level and adding another reason not to use Co foil.

*2.2. Determination of $g'$ and the spin component of magnetization*

The spin component of the magnetization is obtained from experiments measuring what has become known as $g'$, the g-factor obtained from magnetomechanical experiments utilizing fthe Einstein-deHaas effect or the Barnett effect[3]. In general, the $g$-factor is related the to gyromagnetic ratio $\gamma$ of a charged body as

$$\gamma = g\frac{e}{2mc} = g\frac{\mu_B}{\hbar}, \tag{15}$$

where $\mu_B$ is the Bohr magneton[4]. The electron has two g-factors which I will call $g_{sp} \approx 2$ for its spin motion and $g_{orb} = 1$ for its orbital motion. For atoms with angular momentum from orbital motion and spin, $g$ can take on an arbitrary value. This total $g$ for atomic electrons is referred to as $g'$ which is a linear combination of $g_{sp}$ and $g_{orb}$. In publications from the early to middle 1900's, $g_{sp}$ was assumed to be exactly 2 where we now know it to be (up to a sign) the most precisely measured scientific constant $g_{sp} = 2.00231930436182(52)$. In most cases, this 0.1% difference is not consequential, but for the level of precision we are trying to reach for Møller polarimetry, this is not negligible and care must be taken to track down wherever 2 has been substituted for $g_{sp}$. The relationship of $g'$ to the magnetic moment contribution is often given in the literature in the following form [29, 30]

$$g' = \frac{2(M_{sp} + M_{orb})}{M_{sp} + 2M_{orb}} = \frac{2M_{tot}}{M_{tot} + M_{orb}}, \tag{16}$$

where $M_{orb}$, $M_{sp}$ and $M_{tot}$ are the orbital, spin and total magnetic moments respectively. This expression immediately leads to the expression of orbital and spin contributions to the magnetic moment as [3]

$$\frac{M_{orb}}{M_{tot}} = \frac{2 - g'}{g'}, \quad \frac{M_{sp}}{M_{tot}} = 1 - \frac{M_{orb}}{M_{tot}}. \tag{17}$$

[3]The Einstein-deHaas effect (rotation by magnetization) is the rotation of a macroscopic body in a magnetic field when the field is reversed. The Barnett effect (magnetization by rotation) is the converse, the production of a magnetic field by rotation of a macroscopic body.

[4]In early publications sometimes the gyromagnetic ratio is given as $\rho = L/M$ the ratio of the angular momentum to the magnetic moment where at other times it is defined in the usual way as the reciprocal $\gamma = 1/\rho = M/L$.

The derivation of Eq. 16 was first done by Kittel in 1949 in his paper "On the gyromagnetic ration and spectroscopic splitting factor of ferromagnetic substances"[31]. It is helpful to follow through the derivation carefully to ensure that it is intended as an exact not approximate equality. From the definition of gyromagnetic ratio we have $\gamma = M_{tot}/J$, where $M_{tot}$ is the total magnetic moment of the atom and $J = L + S$ is the total angular momentum of the atom. We can now use the relationships $M_{sp} = g_{sp}\mu_B S/\hbar$ and $M_{orb} = g_{orb}\mu_B S/\hbar$ along with Eq. 15 to re-express $\gamma$ in terms of magnetizations as

$$\gamma = g'\frac{\mu_B}{\hbar} = \frac{M_{tot}}{\frac{\hbar}{\mu_B}(M_{sp}/g_{sp} + M_{orb}/g_{orb})}, \tag{18}$$

or simplifying and substituting $g_{orb} = 1$

$$g' = \frac{M_{tot}}{M_{sp}/g_{sp} + M_{orb}} = g_{sp}\frac{M_{tot}}{M_{sp} + g_{sp}M_{orb},} \tag{19}$$

from which we recover Eq. 16 if we substitute $g_{sp} = 2$. Eq. 19 is the exact form which should be used in this analysis. Furthermore, the exact form of Eq. 17 is the slightly more complicated

$$\frac{M_{orb}}{M_{tot}} = \frac{g_{sp} - g'}{g'(g_{sp} - 1)}. \tag{20}$$

This decreases the spin contribution to the total magnetization by 0.11%.

*2.2.1. $g'$ for Fe*

The most precise measurments of $g'$ come from measurements of the gyromagnetic ratio of iron using the Einstein deHaas effect. These magnetomechanical experiments are highly elaborate requiring high precision to observe the tiny effects of interest. The Einstein-deHaas experiments are simple in principle: a sample is suspended from a torsion pendulum along the axis of a magnetic field. Upon reversal of the field a small torque on the sample is measured primarily due to reversal of the valence electron spins. In practice, these experiments are highly technical since the torques on the sample from the Earth's magnetic field are 7-8 orders of magnitude larger than the torques from spin reversal. Elaborate coil setups were utilized to cancel the Earth's field along with any stray magnetic fields in the region and isolation systems incorporated to keep the sample free from interference from outside vibrations. The gyromagnetic ratio was then determined from the ratio of

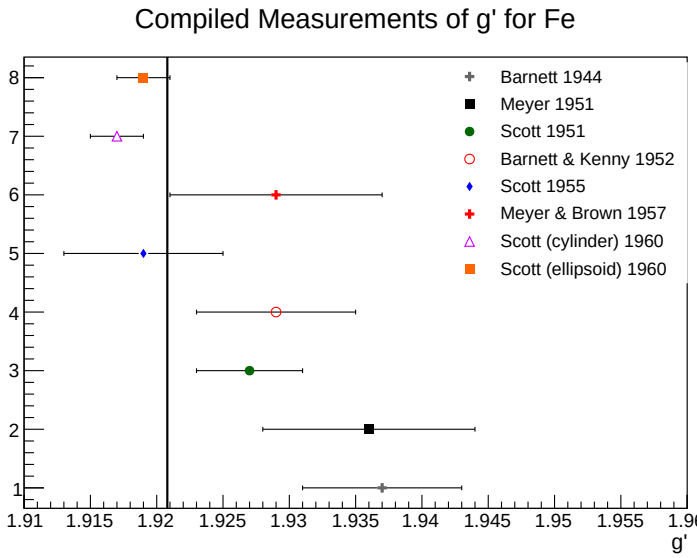


Figure 14: Values of $g'$ for iron as determined by various experiments between 1940 and 1960. The naive constant fit to these data is given by the vertical black line whose value is $g' = 1.9208$.

the angular momentum to the magnetic moment. Similarly complex systems were used in the experiments which measured the Barnett effect. In these experiments a relatively large sample was rotated and the change in magnetic flux measured in a system of pickup coils.

A compilation of $g'$ measurements from magnetomechanical experiments is shown in Fig. 14. These data were taken from compilations in two papers[5] by G. Scott in 1962[32] and Meyer and Asch in 1961[29]. For reference, the data included in these compilations comes from [34, 35, 33, 32]. The final two measurements done by G. Scott are by far the most precise. It is clear that the error bars do not in all cases reflect the actual systematic error. The systematic errors in these experiments are often determined from the re-

[5]There were two inconsistencies between these references[32, 29] which were resolved as follows. Table 1 of [29] has Barnett 1941 $\rho e/mc = 1.035$ whereas Barnett[33] actually had the following 3 values for different Fe samples: 1.032, 1.032 and 1.034. I use the straight average of $\rho e/mc = 1.0327$ or $g' = 1.937 \pm 0.006$ where error is taken from [32]. There is also a discrepancy on the value for Meyer and Brown 1957 between the two papers in which case, of course, I went with the value given by Meyer himself [29] $g' = 1.929 \pm 0.008$, where the error was taken from [32].

peatability of the results. Known systematic effects are canceled or averaged by varying techniques and the systematic error is assigned from remaining differences or instability in the data arising from sources not accounted for. It would appear that the systematic error in at least some of the values is underestimated. Scott, without stated justification, concludes that his most recent measurement of $g' = 1.919 \pm 0.002$ on a prolate ellipsoid sample is the value to use for iron [36, 32] even though he measured $g' = 1.917 \pm 0.002$ on a cylindrical sample using the same apparatus. It is worth noting that his latest value $g' = 1.919$ appears to be the value taken as standard in the literature (see for example [37, 38]). It is far from clear what systematics may be at play here (sample purity, shape, porosity, preparation/annealing process) or which of the measurements closest represents our sample foil. A naive fit using the quoted systematic error bars gives a value $g' = 1.9208$.

For the three samples in used in the measurements $g'$ of Fe, the sample purities were as follows:

- Scott cylinder 99.94% with primary impurities O(0.04%), C(0.005%), N(0.004%), S(0.003%) and Ni(0.0015%) [35]
- Scott ellipsoid, 99.89% with primary impurities Ni(0.05%), Si(0.01%), O(0.005%), Co(0.005%) [36]
- Meyer 1957, 99.9% with primary impurities Mn(0.042%), S(0.029%), Si(0.02%) [39]
- Meyer 1958, 99.99% (negligible impurities) [29].

Scott carefully measured the effect of mixing the ferromagnetic elements Fe, Co and Ni and since their $g'$ values are all within 5% of each other trace amounts of impurities (<1%) from of Ni and Co in Fe will have negligible effect on the value of $g'$ (see Fig 1 of [40]). Furthermore, addition of 3% Si to iron changed the measured g-factor by only 0.5%. We will see in the coming paragraphs that the spectroscopic g-factor is directly related to $g'$ such that if one changes both will. There is little guidance in the literature for the effect of trace amounts of O, Mn, N, C and S on $g'$ for Fe making it difficult to set the scale for such errors. However, Ladislav Pust *et al.* found very little difference in the related quantity spectroscopic $g$ between pure Fe and that with 3% Si by weight. Given the lack of information, the spread in the measurements of different samples provides will be used to estimate the missing systematic error.

An error-weighted fit to these data gives a result of 1.9208±0.0012. However, the $\chi^2$/NDF is 2.96 indicating that systematic errors have been underestimated. Inflating the error bars by 81% yields a fit probability of 0.5 and a fit error of 0.0022.

Related to $g'$ is the spectroscopic $g$-factor often referred to as $g$ from ferromagnetic resonance (FMR) experiments[6]. FMR works by placing a ferromagnetic sample in a resonant microwave cavity. The cavity is placed in a uniform magnetic field at right angles to the direction of propagation of the microwaves. A microwave source feeds the cavity and a detector monitors the energy coming out of the cavity. When the magnetic field is turned on, the magnetic moments of the atoms will begin to precess around the direction of the applied magnetic field with a frequency that depends on the effective magnetic field $H_{eff}$ and the $g$-factor of the sample material material as follows:

$$\hbar\omega = g\mu_B H_{eff} \tag{21}$$

where $H_{eff}$, the effective magnetic field depends on the applied magnetic field strength as well as the magnetization, shape and relative alignment of the specimen (see [31, 30] for a more detailed explanation). The magnetic field strength is then swept over a range until the resonance condition is met where the precession frequency matches that of the microwave cavity. At resonance a drop in power exiting the cavity will be observed due to the energy being absorbed by the sample. Spectroscopic $g$ is determined by measuring the magnetix field which excites this resonance. For a time it was thought that spectroscopic $g$ and $g'$ were the same i.e. that spectroscopic and magnetomechanical experiments were measuring the same $g$-factor until Kittel (1949)[31] and Van Vleck (1950)[41] independently showed that these are distinct although arising from the same physics. In fact, the difference was shown to arise from the contribution of the orbital angular momentum. To a good approximation it can be shown that $g = \frac{2M_{tot}}{M_{tot}-M_{orb}}$ where $g'$ is given approximately by Eq. 16. Thus, the orbital component increases the magnitude of $g$ and decreases $g'$. Using these equations we can easily derive what is known as the Kittel-Van Vleck relationship

$$\frac{1}{g} + \frac{1}{g'} = 1. \tag{22}$$

[6]For a simple explanation of FMR see http://www.physik.fu-berlin.de/einrichtungen/ag/ag-kuch/research/techniques/fmr/index.html

Although this relationship is approximate, it should be good at the 0.1-0.2% level and it has been shown to work quite well in the literature (see for example Fig. 1 of [29]). Therefore, we can utilize spectroscopic measurements of $g$ to check our value of $g'$. Figure 15 shows a compilation of measurements of $g$ for iron. A simple error-weighted fit to these data gives a value of $g = 2.086 \pm 0.004$. Using Eq. 22 gives $g' = 1.9208$ in precise agreement with the error weight fit to $g'$ from magnetomechanical experiments. While we cannot place the same confidence in this derived value of $g'$ as the direct measurements, it does provide a greater level of confidence that determinations from completely different techniques appear to be consistent.

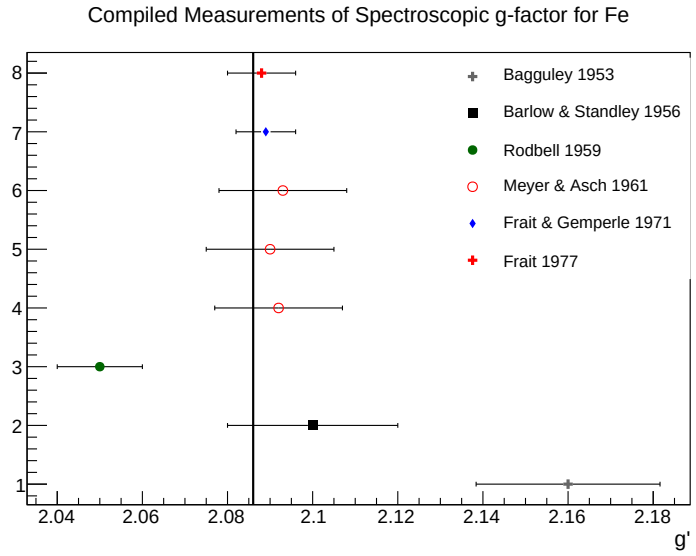


Figure 15: Values of spectroscopic $g$ as determined by various experiments over two decades. The error-weighted fit to these data is given by the vertical black line whose value is $g = 2.086$.

**Recommendation for Fe:** In light of these findings we recommend using the value of the simple error-weighted fit with an inflated systematic error to reflect the tension in the world data: $\mathbf{g' = 1.9208 \pm 0.0022}$. The 0.0022 error comes from inflating the error reported by the fit by the ∼81% required to remove the tension in the data and give a fit probability of 0.5. This places Scott's recommended value of $g' = 1.919 \pm 0.002$ [32] comfortably within $1\sigma$ but almost his earlier measurement almost $2\sigma$ off.

*2.2.2. $g'$ for Ni*

A number of measurements of $g'$ for nickel were performed by A. J. Meyer *et al.*, G. G. Scott *et al.* and S. Barnett *et al.* during the 1950's. At first there were striking differences in the values found for nickel ranging from 1.83 to >1.99. Furthermore, the measurements of spectrocopic $g$ from resonance experiments gave a much lower value of $g'$ using the Eq. 22. A couple of systematic errors in the measurement techniques of both Meyer and Scott were pointed out by Brown which brought the data into much better agreement[32]. However, a considerable inconsistency remained between the measurement of Barnett *et al.* and that of Scott and Meyer. Barnett determined $g' \approx 1.91$ compared to the 0.04% lower $g' \approx 1.84$ found by Meyer and Scott[29, 32]. To investigate the possible reasons for this discrepancy, Meyer measured the Curie temperature and the saturation magnetization of the Ni samples used in each of the measurements. Whereas Scott and Meyer had used nearly pure Ni, Barnett's sample had 1.4% impurities. The presence of these impurities significantly changed the magnetic properties of his Ni sample such that the Curie temperature was reduced from 360°C for pure Ni to 285°C and the saturation magnetization increased from 58.90 to 71.04 (in units of abamp $cm^3/g$)[32]. Scott concludes that this stark shift in magnetic properties makes Barnett's measurements "difficult to retain"[32]. However, this discrepancy provides evidence that the presence of certain impurities can have a significant effect on the measurement of $g'$.

Scott performed a series of four measurements on the same Ni sample in 1952, 1953, 1955 and 1960 and concluded that $g' = 1.835 \pm 0.002$[32]. Meyer *et al.* also measured $g'$ for different Ni samples in 1957 and 1958 finding 1.852±0.010 and 1.845±0.008 [29]. An error-weighted fit to these values gives $g' = 1.836 \pm 0.002$. The impurities in the samples used are as follows:

- Scott: 99.82% Ni with main impurities Si(0.1%), Fe(0.032%), Mn(0.030%), and C(0.01%)[42]
- Meyer, 1957: 99.9% Ni with impurities not provided[39]
- Meyer, 1958: 99.99% with negligible impurities[29]

Looking at the impurities in Scott's sample, we can rule out the effects of Fe and Mn as contributing significantly to a systematic offset using the data in [43, 40]. With carbon impurities at 0.01% this can be considered negligible. Meyer's analysis of the magnetic properties of the Ni sample used

by Scott showed that although the saturation magnetization was changed insignificantly, the Curie temperature decreased by $11°C$. However, no data were located to calibrate the effect Si impurities at 0.1% in Ni even and so a similar approach to that used for the Fe data will be used here. Inflating the error bars on each of the three data points by by 72% gives a best fit of $g' = 1.8362 \pm 0.033$ and a fit probability of 50%.

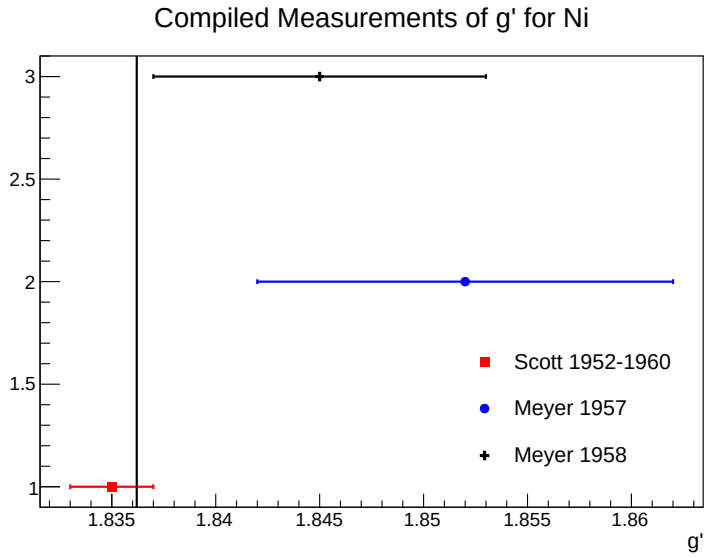


Figure 16: Values of $g'$ for nickel as determined by various experiments between 1950 and 1960. The systematic error on Scott's value as proposed in the text is shown. The error-weighted fit to these data using the proposed error given by the vertical line is $g' = 1.8362 \pm 0.0033$.

Once again we can use measurements of the spectroscopic $g$-factor from magnetic resonance experiments and Eq. 22 as an independent check of our proposed value of $g'$. Table II. of Meyer and Asch [29] provided a compilation of $g$-factors measured in magnetic resonance experiments and concluded that for nickel $g = 2.185 \pm 0.010$ which translates into $g' = 1.844 \pm 0.008$ in good agreement with our proposed value.

**Recommendation for Ni:** In light of these findings we recommend using the value $\mathbf{g' = 1.8362 \pm 0.0033}$ for nickel. The value comes from an error-weighted fit to Scott's and Meyer's measured values after increasing each of the errors by 81% to obtain a fit probability of 50% to accommodate for the underestimated systematic uncertainty. The error quoted is from the

error-weighted fit after inflation.

*2.2.3. Temperature dependence of $g'$*

The measurements of $g'$ used in this analysis have all been at room temperature which is not well-defined but is broadly accepted to be near 20°C give or take a few degrees. Although the target foils in the Møller polarimeter will generally be at room temperature, during measurements with a typical 1-2 $\mu$A of beam on target, the foils will heat up by about 20 degrees Celsius as we saw in Section 2.1.2. This raises the question of whether or not the room temperature values of $g'$ are sufficiently accurate during measurements at elevated temperatures.

In Kittel's 1949 paper on the relation of $g$ and $g'$, he talks about the temperature dependence of $g'$ and suggests there is not enough data to make conclusions[31]. Since then several measurements have been made of $g$ across a broad temperature range for the ferromagnetic elements and alloys. These experiments, which measure $g$ since it is a technically much easier measurement than $g'$, particularly with changing temperatures, are typically at the 1-2% precision level. However, a change in $g$ indicates the inverse change in the $g'$ by Eq. 22. A nice summary of these measurements is found in [44].

It is worth noting that in all cases where pure Ni and Fe were measured, the $g$-factor was always found to be constant within experimental errors, typically at the 1-2% level. However, for alloys, this is not always the case with variations of several percent being observed (see for example [45, 46]).

In two cases extremely accurate measurements were made across a broad temperature range, one for pure Ni and the other for 97% Fe. The first of these was by G. Dewar *et al.* in 1977 on pure nickel foil of 20 $\mu$m thickness. They found $g = 2.187 \pm 0.005$ constant over the temperature range 20-364°C[47]. This constitutes a 0.23% test of temperature dependence over a range much larger than we care about. The second experiment in 1981 by Ladislav Pust and Zdenek Frait measured the $g$-factor of Fe-3wt%Si in the temperature range from 3.5 to 300 K to be constant at $g = 2.0793 \pm 0.0005$[48]. The extreme accuracy of their measurement allowed them to probe the temperature dependence of $g$ at the 0.02% level and they conclude that there is no evidence of temperature dependence across the temperature range they measured. The plot from their paper showing the measurement of $g$ with temperature is shown in Fig. 17. A summary of the various measurements of $g$ is provided in Table 4.

Thus, there is strong evidence that spectroscopic $g$ and by extension $g'$

are, in fact, highly constant for nickel and iron below their Curie temperatures. We conclude that it is safe to proceed with confidence using the room temperature measurements of $g'$ with negligible error.

| Publication | Year | Material | $g$-factor | Temp. (°C) |
|---|---|---|---|---|
| Frait *et al.* [48] | 1981 | Fe-3wt%Si | 2.0793±0.0005 | −270 to 27 |
| Haraldson *et al.* [49] | 1981 | Ni | 2.20±0.02 | 20 to 358 |
| Gadsden *et al.* [45] | 1978 | Ni | 2.20 | −269 to 20 |
| Dewar *et al.* [47] | 1977 | Ni | 2.187±0.005 | 20 to 364 |
| Bastian *et al.* [50] | 1976 | Ni-Fe alloys | const. ±1% | 20 to >300 |
| Rodbell [51] | 1964 | Ni | 2.22±0.03 | −140 to 360 |
| Rodbell [52] | 1959 | Fe | 2.05±0.01 | −196 to 850 |
| Standley *et al.*[43] | 1955 | Ni | 2.17-2.18 | 20 to 200 |
| Bagguley *et al.*[53] | 1954 | Ni | 2.22±0.02 | 20 to 600 |
| Bloembergen [54] | 1950 | Ni | 2.20±1-2% | 24 to 358 |

Table 4: Results of experiments measuring the spectroscopic $g$-factor as a function of temperature for various ferromagnetic materials. Without exception all consider the $g$-factor to be constant within error.

*2.2.4. Magnetic field dependence of $g'$*

In the 1950's while Scott was performing precise measurements of $g'$, he noticed that $g'$ decreased at very low fields and asymptotically approached a larger constant value at higher fields. He published two papers documenting the low-field behavior of $g'$ for nickel and iron[55, 42]. He concluded that the low-field limit for nickel was $g' = 1.873 \pm 0.005$ and its asymptotic value was $g' = 1.919 \pm 0.005$ at higher fields. Incidentally, 1.919 is the same value he later more accurately measured as the value for iron. For nickel he determined the low-field limit to be $g' = 1.801 \pm 0.002$ and the asymptotic value for higher fields to be $g' = 1.830$ with no error estimate provided. He later determined the asymptotic value for nickel to be $g' = 1.835 \pm 0.002$.

Scott apparently considered the asymptotic value to be the true value for all fields higher than the low-field region. He did not specifically give information on the strength of the magnetic field used in his higher field measurements, but piecing together information from his papers, it would

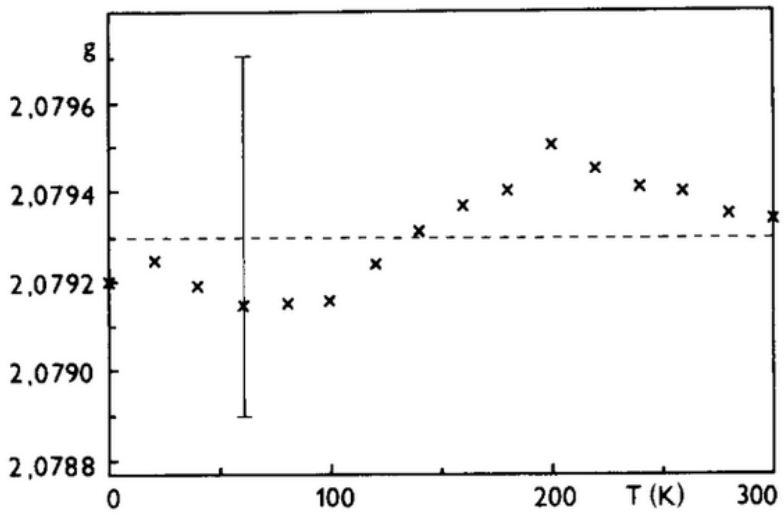


Figure 17: Plot of $g$-values vs. temperature taken from [48]. The vertical bar denotes the accuracy of these values ($\pm 0.0004$).

appear that measurements were all made in the fews tens of Gaus[7]. It is natural to wonder if this value truly is asymptotic or if it changes at high field.

We can again gain insight from FMR measurements of spectroscopic $g$. FMR measurements are made by sweeping the uniform magnetic field strength typically through ranges of order 1 T (see for example Fig. 3 and Table 1 of [54] where the nickel sample is saturated). As noted in Eq. 21, the resonant frequency depends on the magnetization of the sample. Thus, in order to find the $g$-factor, one has to know *a priori* the magnetization of the sample. For ferromagnetic elements, the saturation magnetization is well-determined from the literature and is repeatable i.e. there is a single saturation magnetization value for a given field and temperature. There-

[7]To estimate the applied magnetic field in Scott's experiments I assumed from the drawing in figure 4 of [32] that the magnetic coil was about the same size as the nickel and iron cylindrical samples which were 22 cm long and 1.5 cm in diameter. The "winding constant" of the coil was about 78,500 cm$^2$, which I divided by the cross-sectional area and the length to get the number of turns per meter n$\approx$2000. The maximum current through the coil appears to be 16 mA which makes the applied field $H = \mu_0 nI \approx 4$ mT=40 G.

fore, these measurements are taken with a saturated sample. We can this consider these to be high-field measurements of the $g$-factor. Furthermore, many FMR measurements take data at multiple frequencies requiring a range of magnetic fields for the different resonance frequencies.

In 1971, Z. Frait and R. Gemperle measured the $g$-factor of single iron crystals across a range of frequencies from 12 to 70 GHz requiring a broad range of static magnetic fields which I estimate to be from 0.1 T to higher than 1.5 T. They found that $g = 2.089 \pm 0.007$ and that it is frequency independent over this range within their experimental error, constituting a $\sim$0.3% test of the field dependence of $g$[56]. In 1977, Z. Frait published an FMR measurement of $g = 2.088 \pm 0.008$ for pure polycrystalline iron at three frequencies, 26 GHz (at 0.32 T), 36 GHz (at 0.57 T) and 70 GHz (at 1.53 T)[57]. Once again he concluded that within experimental error this value is frequency independent. This constitutes a 0.4% high-field test of field dependence on $g$ on iron. Taken together these constitute a 0.25% test of the field dependence of $g$ on iron. In addition, the 0.024% measurement of the $g$-factor of Fe-3wt%Si by Pust *et al.* was accomplished by averaging measurements at four different frequencies, 36 GHz, 70 GHz, 86 GHz and 95 GHz[48]. Information in a later paper shows that their electromagnet was capable of creating fields as high as 3 T which sets the scale of the range of these measurements[58]. They averaged their measurements taken at the four different frequencies (and by extension magnetic fields) to obtain the final result. Although no specific statement is made about the frequency independence of these measurements, the fact that the values were averaged and a tiny error assigned seems to point to a small or non-existent systematic frequency dependence. Finally, we can connect these observations of the field-independence of $g$ with $g'$ using Eq. 22 to conclude that within the error of the experimental data available $g$ and $g'$ appear to be field-independent at least in fields high enough to saturate the sample. Furthermore, the value of $g'$ for iron derived from high-field measurements of $g$ agrees well with the low field direct measurements of $g'$ consistent with the determination of Scott that $g'$ asymptotically approaches the low-field value he measured.

For nickel the data are less precise but point to the same conclusion that $g$ is field-independent. In 1950 Bloembergen measured the $g$-factor of nickel to be 2.23 at 9.05 GHz with a field of 0.116 T and 2.24 at 22.44 GHz with a magnetic field of 0.54 T. These values are equal within the error of the experiment. In 1959, Rodbell found that for nickel $g$ was constant at the 0.5% level over a range of magnetic fields up to 0.3 T[52]. In 1965, Frait

found that $g$ was independent of frequency for pure nickel at the 2% level over a range of frequencies from 8.5 GHz to 72 GHz. He also found that an alloy consisting of 42% Fe and 58% Ni was independent of frequency over the same range at the 1% level. Although the field range is not given, we estimate the range to be as high as 1.5 T. Finally, as we saw earlier in Section 2.2.3 the value of $g'$ for nickel derived from high-field measurements of $g$ agrees well within error with the direct measurements at low field, providing further evidence of the validity of the asymptotic value of $g'$ for nickel.

Using Eq. 22 to interpret the independence of $g$ on applied field as also applying to $g'$, we argue there is no evidence of $g'$ depending on magnetic field at the 0.25% level for pure Fe. Combining this with what appears to be the lack of frequency dependence in Fe-3wt%Si for extremely accurate measurements provides confidence that the asymptotic direct measurements of $g'$ for iron measured at comparatively low fields are valid for the relatively high fields of several Tesla using in the Hall A Møller polarimeter. For nickel the value of $g$ is not known as accurately so the comparison between $g'$ derived from high-field values of $g$ and the low field measurements of $g'$ suffer from $\sim$0.5% level uncertainties. Within this level of uncertainty $g'$ does not appear to depend on magnetic field. Without evidence to the contrary it seems reasonanle to assume that the asymptotic measurements of $g'$ at lower field are truly asymptotic and not further systematic error is needed to account for field dependence.

## 3. Calculation of Target Polarization

We are now in a position to calculate the final target polarization and the uncertainty on the value. Tables 5 and 6 provide the path to final target polarization from the measured values of saturation magnetization and $g'$ for Fe and Ni respectively. The values for magnetization and polarization are calculated for applied magnetic fields of 4 T and 2 T for Fe and Ni foils respectively. In the calculation of target polarization by deBever *et al.* in [3] an equivalence is drawn between target electron polarization and the average electron magnetic moment. This is an approximation valid in the limit that $g_{sp} = 2$ and introduces an error at the 0.1% level. The calculation is as follows:

$$\hat{\mu} = g_{sp}\frac{e}{2m_e}\hat{S}_z = g_{sp}\mu_B\frac{1}{\hbar}\hat{S}_z.$$

Substituting the eigenvalues of spin $S_z = \pm\hbar/2$ gives

$$\mu = \pm\frac{g_{sp}}{2}\mu_B.$$

Thus the spin of an electron is approximately $1.00116\mu_B$.

Temperature corrections due to target heating are calculated for a 1 $\mu$A beam load. To first order increasing the beam load linearly increases the temperature correction whereas increasing target thickness leaves the temperature unchanged. Therefore, increasing foil thickness is the better choice for higher scattering rates.

| Quantity | T=294 K | T=305 K | Unit |
|---|---|---|---|
| Saturation magnetization $M_s$ | 218.02(44) | 217.76(45) | emu/g |
| Saturation magnetization $M_s$ | 2.1800(44) | 2.1774(45) | $\mu_B$/atom |
| $g'$ | 1.9208(22) | 1.9208(22) | – |
| Orbital fraction: $\frac{M_{orb}}{M_{total}} = \frac{g_{sp}-g'}{g'(g_{sp}-1)}$ | 0.0423(12) | 0.0423(12)) | – |
| Spin component: $M_s\left(1-\frac{M_{orb}}{M_{tot}}\right)$ | 2.0877(50) | 2.0852(50) | $\mu_B$/atom |
| Average electron magnetization | 0.08030(19) | 0.08020(19) | $\mu_B$ |
| Average electron polarization | 0.08020(19) | 0.08011(19) | – |

Table 5: Summary of values and errors involved in calculating the target polarization for Fe foils. The ratio of electron magnetization in Bohr magnetons and electron polarization is $g_{sp}/2 \approx 1.00116$ not unity as supposed in [3].

It is important to verify at the <0.1% level that the target indeed is saturated at the final magnetic field settings. Diagrams such as Figs. 1 and 2 in [3] imply that a perfectly aligned foil will saturate out-of-plane at 2.2 T, which is the saturation magnetization of Fe and that if it does not thenalignment is the most likely issue. However, numerous other effects such as "impurities, strains, anisoptropic contributions, geometric effects etc." prevent saturation [59]. Foner *et al.* found for an Fe foil that "although the saturation value of $H_{DM}$[8] is 21.8 kG, because of the anisotropy energy associated with the rotation of domains and the movement of domains boundaries, we have

[8] $H_{DM}$ is the demagnetizing field which for the case of a thin iron foil magnetized out of plane is $4\pi M = 21.8$ kG = 2.18 T.

| Quantity | T=294 K | T=305 K | Unit |
|---|---|---|---|
| Saturation magnetization $M_s$ | 55.24(11) | 54.97(14) | emu/g |
| Saturation magnetization $M_s$ | 0.5805(12) | 0.5776(14) | $\mu_B$/atom |
| $g'$ | 1.8362(33) | 1.8362(33) | – |
| Orbital fraction: $\frac{M_{orb}}{M_{total}} = \frac{g_{sp}-g'}{g'(g_{sp}-1)}$ | 0.0903(20) | 0.0903(20)) | – |
| Spin component: $M_s\left(1-\frac{M_{orb}}{M_{tot}}\right)$ | 0.5281(15) | 0.5255(17) | $\mu_B$/atom |
| Average electron magnetization | 0.018862(55) | 0.018768(62) | $\mu_B$ |
| Average electron polarization | 0.018840(55) | 0.018746(62) | – |

Table 6: Summary of values and errors involved in calculating the target polarization for Ni foils.

experimentally determined that fields of the order of 30 kG applied perpendicular to the plane of the iron foil are necessary to align completely the magnetization along the external field direction"[59].

## 4. Concluding Discussion

The polarization of a saturated ferromagnetic target has been calculated for both nickel and iron foils. With the stringent demands of the proposed MOLLER experiment, it seemed wise to revisit the study of Fe target polarization by deBever *et al.*[3]. A different approach was taken than that in [3] where instead of using the saturation magnetization value at 0 K and then correcting back to room temperature, measured values of magnetization were taken at or near room temperature. A small error was found in the magnetic field correction in equation (3) of [3] where the applied magnetic field was used instead of the internal magnetic field, introducing a small error of about 0.1%. A couple of approximations also introduced further errors of order 0.1% in [3]. These were as follows:

1). The expression $M_{orb}/M_{tot} = (2 - g')/g'$ used to calculate the orbital and spin components of the magnetization is an approximate expression which more accurately is given by Eq. 19.

2). The equating of electron target polarization and average electron magnetization in units of $\mu_B$ is true only in the approximation $g'/2 = 1$.

The error in target polarization listed in the MEI proposal for the MOLLER experiment was 0.25%. This study concludes that the polarization at room temperature of an ideal (perfectly flat, high purity, aligned precisely normal to the holding field) saturated Fe foil is known to $\pm 0.20\%$ and that of a Ni foil to $\pm 0.29\%$. This applies to fields in the vicinity of 4 T for Fe foils and 2 T for Ni foils. Additional uncertainty associated with the temperature correction under a 1 $\mu$A electron beam load takes adds negligible uncertainty for Fe but increases the relative uncertainty for Ni to $\pm 0.34\%$. The relatively low Curie temperature of Ni makes it much more sensitive to temperature corrections. Recent evidence from measurement in Hall A revealed our sensitivity to wrinkles in the foil and raised questions about how well our foils were aligned normal to the holding field. Deviations of the foil surface from normality make it more difficult to reach saturation which is the only place where polarization is known with high accuracy. Further studies will be needed and are ongoing to determine the level of foil flatness required and our sensitivity to foil alignment angle. To reach the proposed uncertainty of 0.25% for foil polarization, uncertainties from foil alignment and flatness must be limited such that we are confident that we are within $\pm 0.08\%$ of saturation.

## References


[1] T. M. Collaboration", The moller experiment: An ultra-precise measurement of the weak mixing angle using mller scattering (2014). arXiv:1411.4088.

[2] T. S. collaboration, Solid (solenoidal large intensity device) updated preliminary conceptial design report (Nov 2019).
URL https://hallaweb.jlab.org/12GeV/SoLID/files/solid-precdr-Nov2019.pdf

[3] L. de Bever, J. Jourdan, M. Loppacher, S. Robinson, I. Sick, J. Zhao, A target for precise Møller polarimetry, Nuclear Instruments and Methods in Physics Research Section A: Accelerators, Spectrometers, Detectors and Associated Equipment 400 (2) (1997) 379 – 386. doi:http://dx.doi.org/10.1016/S0168-9002(97)00961-3.
URL http://www.sciencedirect.com/science/article/pii/S0168900297009613

[4] M. Swartz, H. Band, F. Decker, P. Emma, M. Fero, R. Frey, R. King, A. Lath, T. Limberg, R. Prepost, P. Rowson, B. Schumm, M. Woods, M. Zolotorev, Observation of target electron momentum effects in single-arm mller polarimetry, Nuclear Instruments and Methods in Physics Research Section A: Accelerators, Spectrometers, Detectors and Associated Equipment 363 (3) (1995) 526 – 537. doi:https://doi.org/10.1016/0168-9002(95)00384-3.
URL http://www.sciencedirect.com/science/article/pii/0168900295003843

[5] F. Bloch, Zur theorie des ferromagnetismus, Zeitschrift für Physik 61 (3) (1930) 206–219. doi:10.1007/BF01339661.
URL http://dx.doi.org/10.1007/BF01339661

[6] R. Pauthenet, Experimental verification of spinwave theory in high fields (invited), Journal of Applied Physics 53 (11) (1982) 8187–8192. doi:10.1063/1.330287.
URL http://dx.doi.org/10.1063/1.330287

[7] R. Pauthenet, Spinwaves in nickel, iron, and yttriumiron garnet, Journal of Applied Physics 53 (3) (1982) 2029–2031. doi:10.1063/1.330694.
URL http://dx.doi.org/10.1063/1.330694

[8] C. D. G. Jr., Iron and nickel as magnetization standards, Journal of Applied Physics 53 (3) (1982) 2032–2034. doi:10.1063/1.330695.
URL http://dx.doi.org/10.1063/1.330695

[9] E. A. Owen, D. M. Jones, Effect of grain size on the crystal structure of cobalt, Proceedings of the Physical Society. Section B 67 (6) (1954) 456.
URL http://stacks.iop.org/0370-1301/67/i=6/a=302

[10] W. E. Case, R. D. Harrington, Calibration of vibrating-sample magnetometers, Journal of Research of the National Bureau of Standards-C Engineering and Instrumentation 70C (4) (1966) 255–262.
URL http://nvlpubs.nist.gov/nistpubs/jres/70C/jresv70Cn4p255_A1b.pdf

[11] J. Crangle, G. M. Goodman, The magnetization of pure iron and nickel, Proceedings of the Royal Society of London A: Mathematical, Physical and Engineering Sciences 321 (1547) (1971) 477–491. doi:10.1098/rspa.1971.0044.
URL http://rspa.royalsocietypublishing.org/content/321/1547/477

[12] H. Danan, A. Herr, A. J. P. Meyer, New determinations of the saturation magnetization of nickel and iron, Journal of Applied Physics 39 (2) (1968) 669–670. doi:10.1063/1.2163571.
URL http://dx.doi.org/10.1063/1.2163571

[13] A. T. Aldred, Temperature dependence of the magnetization of nickel, Phys. Rev. B 11 (1975) 2597–2601. doi:10.1103/PhysRevB.11.2597.
URL https://link.aps.org/doi/10.1103/PhysRevB.11.2597

[14] Weiss, Pierre, Forrer, R., La saturation absolue des ferromagntiques et les lois d'approche en fonction du champ et de la temprature, Ann. Phys. 10 (12) (1929) 279–372. doi:10.1051/anphys/192910120279.
URL https://doi.org/10.1051/anphys/192910120279

[15] R. L. Sanford, E. G. Bennett, A determination of the magnetic saturation induction of iron at room temperature, NIST Journal of Research.
URL http://nistdigitalarchives.contentdm.oclc.org/cdm/ref/collection/p13011coll6/id/104774

[16] H. Danan, On the interpretation of the magnetization measurements of pure polycrystalline iron and nickel in the vicinity of saturation, J. Phys. Radium 20 (2-3) (1959) 203–207. doi:10.1051/jphysrad:01959002002-3020300.
URL https://hal.archives-ouvertes.fr/jpa-00236018

[17] S. Arajs, G. R. Dunmyre, A note on the consistency of values of the spontaneous or saturation magnetization of polycrystalline iron and nickel at 298 k, physica status solidi (b) 21 (1) (1967) 191–195. doi:10.1002/pssb.19670210117.
URL http://dx.doi.org/10.1002/pssb.19670210117

[18] D. R. Behrendt, D. E. Hegland, Saturation magnetization of polycrystalline iron, Tech. rep., NASA (Apr 1972).
URL https://ntrs.nasa.gov/search.jsp?R=19720015089

[19] C. S. Edmund, Ferromagnetism: magnetization curves, Reports on Progress in Physics 13 (1) (1950) 83–183. doi:10.1088/0034-4885/13/1/304.
URL https://doi.org/10.1088/0034-4885/13/1/304

[20] S. Foner, Hall effect and magnetic properties of armco iron, Phys. Rev. 101 (1956) 1648–1652. doi:10.1103/PhysRev.101.1648.
URL https://link.aps.org/doi/10.1103/PhysRev.101.1648

[21] B. D. Cullity, C. D. Graham, Introduction to Magnetic Materials, 2nd Edition, Wiley-IEEE Press, 2008.

[22] H. P. Myers, W. Sucksmith, The spontaneous magnetization of cobalt, Proceedings of the Royal Society of London A: Mathematical, Physical and Engineering Sciences 207 (1091) (1951) 427–446. arXiv:http://rspa.royalsocietypublishing.org/content/207/1091/427.full.pdf, doi:10.1098/rspa.1951.0132.
URL http://rspa.royalsocietypublishing.org/content/207/1091/427

[23] S. Arajs, R. V. Colvin, Ferromagneticparamagnetic transition in iron, Journal of Applied Physics 35 (8) (1964) 2424–2426. doi:10.1063/1.1702873.
URL http://dx.doi.org/10.1063/1.1702873

[24] S. Arajs, R. Colvin, Paramagnetism of polycrystalline nickel, Journal of Physics and Chemistry of Solids 24 (10) (1963) 1233 – 1237. doi:http://dx.doi.org/10.1016/0022-3697(63)90242-7.
URL http://www.sciencedirect.com/science/article/pii/0022369763902427

[25] S. Arajs, Paramagnetic behavior of nickel just above the ferromagnetic curie temperature, Journal of Applied Physics 36 (3) (1965) 1136–1137. doi:10.1063/1.1714136.
URL http://dx.doi.org/10.1063/1.1714136

[26] F. E. Luborsky, J. L. Walter, E. P. Wohlfarth, The saturation magnetisation, curie temperature and size effect of amorphous iron alloys, Journal of Physics F: Metal Physics 10 (5) (1980) 959.
URL http://stacks.iop.org/0305-4608/10/i=5/a=024

[27] S. A. Ahern, M. J. C. Martin, W. Sucksmith, The spontaneous magnetization of nickel+copper alloys, Proceedings of the Royal Society of London. Series A, Mathematical and Physical Sciences 248 (1253) (1958) 145–152.
URL http://www.jstor.org/stable/100593

[28] P. R. Locher, S. Geschwind, Electron-nuclear double resonance of $fe^{57}$ in mgo, Phys. Rev. 139 (1965) A991–A994. doi:10.1103/PhysRev.139.A991.
URL https://link.aps.org/doi/10.1103/PhysRev.139.A991

[29] A. J. P. Meyer, G. Asch, Experimental g and g values of fe, co, ni, and their alloys, Journal of Applied Physics 32 (3) (1961) S330–S333. doi:10.1063/1.2000457.
URL http://dx.doi.org/10.1063/1.2000457

[30] J. Smit, H. Wijn, Ferrites, Eindhoven: Philips Technical Library, 1959.

[31] C. Kittel, On the gyromagnetic ratio and spectroscopic splitting factor of ferromagnetic substances, Phys. Rev. 76 (1949) 743–748. doi:10.1103/PhysRev.76.743.
URL https://link.aps.org/doi/10.1103/PhysRev.76.743

[32] G. G. Scott, Review of Gyromagnetic Ratio Experiments, Reviews of Modern Physics 34 (1962) 102–109. doi:10.1103/RevModPhys.34.102.

[33] S. J. Barnett, G. S. Kenny, Gyromagnetic ratios of iron, cobalt, and many binary alloys of iron, cobalt, and nickel, Phys. Rev. 87 (1952) 723–734. doi:10.1103/PhysRev.87.723.
URL https://link.aps.org/doi/10.1103/PhysRev.87.723

[34] S. J. Barnett, New researches on magnetization by rotation and the gyromagnetic ratios of ferromagnetic substances, Proceedings of the American Academy of Arts and Sciences 75 (5) (1944) 109–129.
URL http://www.jstor.org/stable/20023462

[35] G. G. Scott, A precise mechanical measurement of the gyromagnetic ratio of iron, Phys. Rev. 82 (1951) 542–547. doi:10.1103/PhysRev.82.542.
URL https://link.aps.org/doi/10.1103/PhysRev.82.542

[36] G. G. Scott, Gyromagnetic ratios of fe and ni, Phys. Rev. 119 (1960) 84–85. doi:10.1103/PhysRev.119.84.
URL https://link.aps.org/doi/10.1103/PhysRev.119.84

[37] E. Wohlfarth, Chapter 1 iron, cobalt and nickel, Handbook of Ferromagnetic Materials 1 (1980) 35. doi:http://dx.doi.org/10.1016/S1574-9304(05)80116-6.
URL http://www.sciencedirect.com/science/article/pii/S1574930405801166

[38] D. Bonnenberg, K. A. Hempel, H. Wijn, 1.2.1.2.4 Atomic magnetic moment, magnetic moment density, g and g' factor, Springer Berlin Heidelberg, Berlin, Heidelberg, 1986, pp. 174–188. doi:10.1007/10311893_25.
URL https://doi.org/10.1007/10311893_25

[39] Meyer, Andr J.P., Brown, Sheldon, Nouvelles mesures des rapports gyromagntiques du fer et du nickel, J. Phys. Radium 18 (3) (1957) 161–168. doi:10.1051/jphysrad:01957001803016100.
URL https://doi.org/10.1051/jphysrad:01957001803016100

[40] G. G. Scott, H. W. Sturner, Magnetomechanical ratios for fe-co alloys, Phys. Rev. 184 (1969) 490–491. doi:10.1103/PhysRev.184.490.
URL https://link.aps.org/doi/10.1103/PhysRev.184.490

[41] J. H. Van Vleck, Concerning the theory of ferromagnetic resonance absorption, Phys. Rev. 78 (1950) 266–274. doi:10.1103/PhysRev.78.266.
URL https://link.aps.org/doi/10.1103/PhysRev.78.266

[42] G. G. Scott, Gyromagnetic ratio of nickel at low magnetic intensities, Phys. Rev. 99 (1955) 1824–1825. doi:10.1103/PhysRev.99.1824.
URL https://link.aps.org/doi/10.1103/PhysRev.99.1824

[43] K. J. Standley, K. H. Reich, Ferromagnetic resonance in nickel and in some of its alloys, Proceedings of the Physical Society. Section B 68 (10) (1955) 713.
URL http://stacks.iop.org/0370-1301/68/i=10/a=303

[44] A. Borovik-Romanov, S. Sinha, Spin Waves and Magnetic Excitations, no. pt. 2 in Modern problems in condensed matter sciences, North-Holland, 1988.
URL https://books.google.com/books?id=Qj9BAQAAIAAJ

[45] C. J. Gadsden, M. Heath, Ferromagnetic resonance of nickel vanadium alloys, Journal of Physics F: Metal Physics 8 (3) (1978) 521.
URL http://stacks.iop.org/0305-4608/8/i=3/a=021

[46] B. D. Shanina, V. G. Gavriljuk, A. A. Konchits, S. P. Kolesnik, The influence of substitutional atoms upon the electron structure of the iron-based transition metal alloys, Journal of Physics: Condensed Matter 10 (8) (1998) 1825.
URL http://stacks.iop.org/0953-8984/10/i=8/a=015

[47] G. Dewar, B. Heinrich, J. F. Cochran, Ferromagnetic antiresonance transmission of 24ghz radiation through nickel (20 to 364 c), Canadian Journal of Physics 55 (9) (1977) 821–833. doi:10.1139/p77-112.
URL https://doi.org/10.1139/p77-112

[48] L. Pst, Z. Frait, Precise g-factor determination of fe3wtrange 3.5300 k by electron fmr and fmar measurements, Physics Letters A 86 (1) (1981) 48 – 50. doi:http://dx.doi.org/10.1016/0375-9601(81)90685-X.
URL http://www.sciencedirect.com/science/article/pii/037596018190685X

[49] S. Haraldson, L. Pettersson, Ferromagnetic resonance in nickel around the curie temperature, Journal of Physics and Chemistry of Solids 42 (8)

(1981) 681 – 686. doi:http://dx.doi.org/10.1016/0022-3697(81)90121-9.
URL http://www.sciencedirect.com/science/article/pii/0022369781901219

[50] D. Bastian, E. Biller, Anisotropy constants and g-factors of nife alloys derived from ferromagnetic resonance, physica status solidi (a) 35 (2) (1976) 465–470. doi:10.1002/pssa.2210350207.
URL http://dx.doi.org/10.1002/pssa.2210350207

[51] D. S. Rodbell, Ferromagnetic resonance absorption linewidth of nickel metal. evidence for landau-lifshitz damping, Phys. Rev. Lett. 13 (1964) 471–474. doi:10.1103/PhysRevLett.13.471.
URL https://link.aps.org/doi/10.1103/PhysRevLett.13.471

[52] D. S. Rodbell, Ferromagnetic resonance of iron whisker crystals, Journal of Applied Physics 30 (4) (1959) S187–S188. doi:10.1063/1.2185880.
URL http://dx.doi.org/10.1063/1.2185880

[53] D. M. S. Bagguley, N. J. Harrick, The temperature dependence of ferromagnetic resonance in colloidal nickel, Proceedings of the Physical Society. Section A 67 (7) (1954) 648.
URL http://stacks.iop.org/0370-1298/67/i=7/a=115

[54] N. Bloembergen, On the ferromagnetic resonance in nickel and supermalloy, Phys. Rev. 78 (1950) 572–580. doi:10.1103/PhysRev.78.572.
URL https://link.aps.org/doi/10.1103/PhysRev.78.572

[55] G. G. Scott, Gyromagnetic ratio of iron at low magnetic intensities, Phys. Rev. 99 (1955) 1241–1244. doi:10.1103/PhysRev.99.1241.
URL https://link.aps.org/doi/10.1103/PhysRev.99.1241

[56] FRAIT, Z., GEMPERLE, R., The g-factor and surface magnetization of pure iron along [100] and [111] directions, J. Phys. Colloques 32. doi:10.1051/jphyscol:19711182.
URL https://doi.org/10.1051/jphyscol:19711182

[57] Z. Frait, The g-factor in pure polycrystalline iron, Czechoslovak Journal of Physics B 27 (2) (1977) 185–189. doi:10.1007/BF01587010.
URL https://doi.org/10.1007/BF01587010

[58] L. Pst, Z. Frait, Low-temperature fmr and fmar measurements of metal single crystals. i. general consideration, experimental techniques, physica status solidi (b) 122 (2) (1984) 535–541. doi:10.1002/pssb.2221220218.
URL http://dx.doi.org/10.1002/pssb.2221220218

[59] S. Foner, A. J. Freeman, N. A. Blum, R. B. Frankel, E. J. McNiff, H. C. Praddaude, High-field studies of band ferromagnetism in fe and ni by mössbauer and magnetic moment measurements, Phys. Rev. 181 (1969) 863–882. doi:10.1103/PhysRev.181.863.
URL https://link.aps.org/doi/10.1103/PhysRev.181.863